DECO Electronics, Inc.

Boston Boulder Leesburg Washington

DEEP EARTH CONDUCTIVITY

MEASUREMENT TECHNIQUES

REPORT NO. 30-P-10

AUTHORS:

J. J. Jacobson

E. L. Maxwell

January 1966

Navy Department

Office of Naval Research

Washington, D.C.

Contract NOnr 3387(00) Nr. 371-590 Dated: 15 December 1960

COPY NO. 23

DECO ELECTRONICS, INC.

BOSTON BOULDER LEESBURG WASHINGTON, D.C.

TABLE OF CONTENTS

Section		Page
1	INTRODUCTION.	1
2	ELECTRICAL GEOPHYSICAL METHODS.	2
3	DECO FIELD OPERATIONS.	11
	3.1 Field Procedures	11
	3.2 Instrumentation Used	12
	3.3 Audio System	12
	3.4 Deep Probe System	12
4	CONCLUSIONS	20
5	REFERENCES	21
	APPENDIX A	A-1

LIST OF ILLUSTRATIONS

Figure	Title	Page
1	Four-Terminal Array Configuration.	4
2	Audio Sounding Equipment	13
3	Deep Probe Equipment.	14
4a	Sample of Deep Probe Records	17
4b	Sample of Deep Probe Records	17
4c	Sample of Deep Probe Records	18

ABSTRACT

Since 1960 DECO Electronics, Inc. has obtained considerable experience in the technique of measuring the electrical conductivity of the earth. This report deals specifically with the four-terminal array methods, their underlying theory and interpretation procedures. Field techniques for concentrated shallow surveys or deep crustal surveys are given. The instrumentation for the shallow surveys consists of commercially available components, whereas the equipment for the deep measurements was designed and built by DECO.

The appendix to this report, A Manual for the Interpretation of Layered Conductivity Curves for the Sequence High-Low-High, by Dr. G. V. Keller, discusses in detail many of the problems associated with the real earth in contrast to the idealized earth for which most of the theory has previously been developed. Theoretical curves for several two and three layer cases, effective spacing curves and cross dipole curves are included in the set of curves.

1. INTRODUCTION

Increased interest in subsurface communications*, Mohorovicic discontinuity studies, ELF phenomena, etc. has spotlighted a lack of data relative to the electrical properties of the earth's crust at great depth. Surface conductivities for broadcast frequencies have been given by Fine [1954], and near surface conductivities for VLF have been recently reported by Morgan and Maxwell [1965]. The depth of the mantle and its conductivity has been studied by the magnetic field and telluric current variations as reported in the survey paper by Watt, Mathews, and Maxwell [1963]. These methods did not yield the conductivity of the deep crust itself. The masking effect of thick, high conductivity sedimentary layers reduced the effectiveness of much of this early work. Four terminal array measurements coupled with recent improvements in current supplies and voltage measuring techniques have made conductivity measurements to depths of tens of kilometers possible. This in turn has necessitated refinements in interpretation methods. Some of the more elementary interpretation methods are discussed as well as the equipment used in obtaining four terminal array data.

*See IEEE Transactions on Antennas and Propagation, Vol. AP-11, No. 3, May 1963

2. ELECTRICAL GEOPHYSICAL METHODS

Electrical earth measurements are more diversified than any other geophysical method. Some of the measurement techniques depend on natural electric and magnetic fields (such as spontaneous-polarization and magnetotelluric techniques) whereas others measure the fields from currents artificially introduced into the earth. Some of the techniques measure the effective conductivity of the earth at the frequency used. Others measure the apparent conductivity at d. c. and low frequencies.

The four-terminal array method uses man-made currents and determines the apparent low frequency or d. c. conductivity as a function of array geometry. The field data is interpreted in terms of a layered earth having specific layer thicknesses and conductivities. This in turn can be used to calculate an effective conductivity at the frequency of interest.

DECO chose to use this technique for the following reasons:

(1) The technique is well established and the interpretation of data well known. It has been used for geophysical exploration for over 30 years.

(2) In contrast to other techniques, data is obtained from the surface (the first few feet) continuously to depths limited only by the equipment (in this case 30 - 70 km). This results in a complete analysis of conductivity vs. depth and effective conductivity for frequencies from MF down, the lower frequency limit being established by the skin depth and maximum sounding depth.

(3) The results from this technique have been found to agree with geologic data (from drill holes and other observations) and with data obtained using other more limited techniques.

Only the four-terminal array technique will be discussed in detail in this report.

Four-terminal arrays consist of four electrodes placed in the earth. Two electrodes feed current into the earth and two electrodes measure the

induced potential. Orientation of the electrodes is quite arbitrary. Certain arrangements are most useful for specific tasks, however, and lend themselves to convenient field deployment. The most common arrays are Wenner, Eltran Schlumberger, and Dipole (see Figure 1). The development of the relationship between current, I, induced potential, V, electrode spacings and apparent conductivity, σ_a, begins with Maxwell's field equations for a dc field. This development for the common arrays is given by Keller and Frischknecht [1965], and Wait and Conda [1958] and will not be repeated here. The results are given below:

WENNER ARRAY

$$\sigma_a = \frac{I}{2\pi a V} \qquad (1)$$

ELTRAN ARRAY

$$\sigma_a = \frac{I}{6\pi a V} \qquad (2)$$

SCHLUMBERGER ARRAY

$$\sigma_a = \frac{2aI}{\pi b^2 V} \qquad (3)$$

GENERAL DIPOLE ARRAY

$$\sigma_a = \frac{Iac}{\pi b^3 V} \left| \cos\theta \cos(\beta) + (1/2)\sin\theta \sin(\beta) \right| \qquad (4)$$

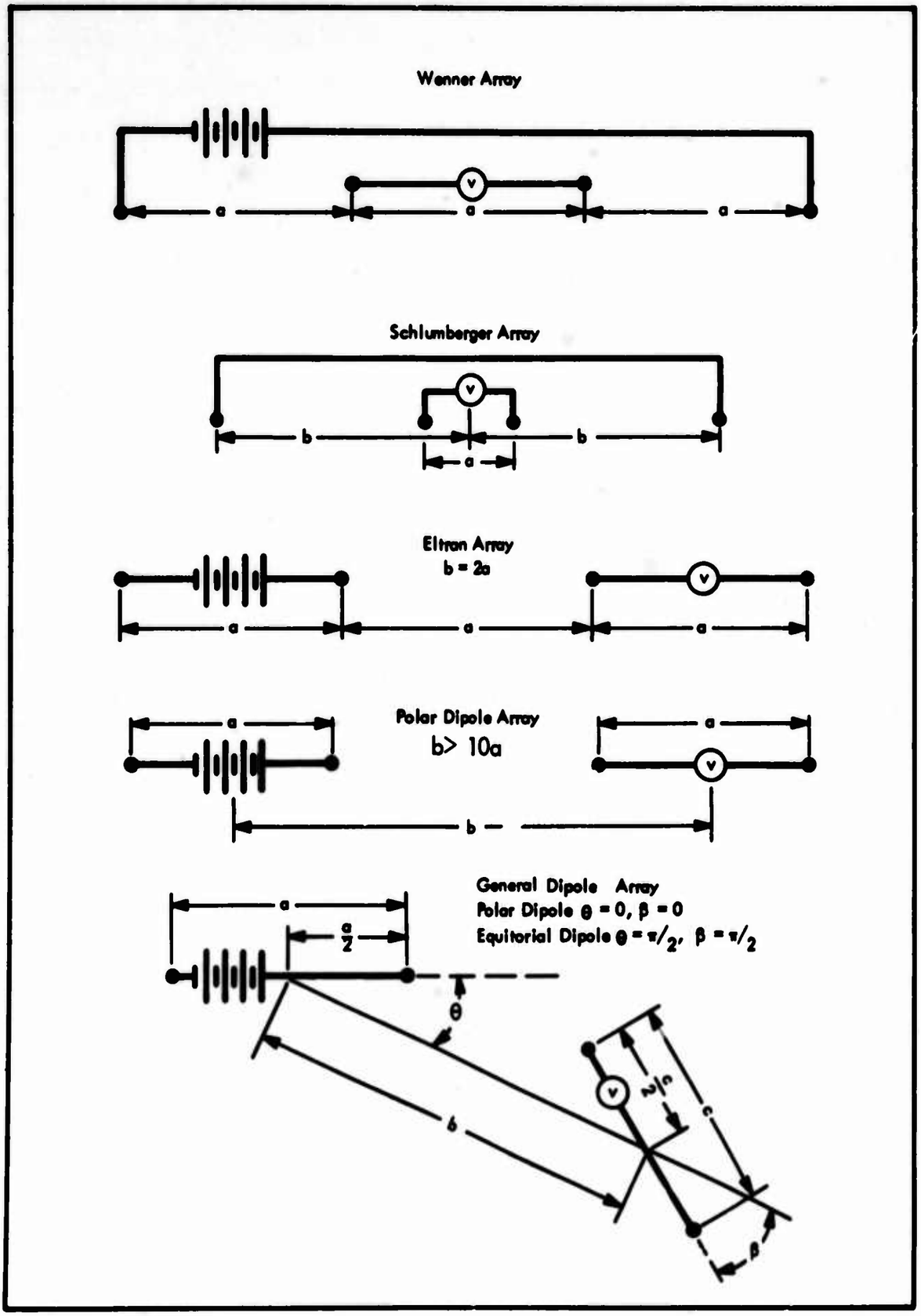

Figure 1 Four-Terminal Array Configurations

IN LINE (POLAR) DIPOLE ARRAY ($\theta = \beta = 0°$)

$$\sigma_a = \frac{I a c}{\pi b^3 V} \tag{5}$$

BROADSIDE (EQUATORIAL) DIPOLE ARRAY ($\theta = 90°, \beta = 90°$)

$$\sigma_a = \frac{I a c}{2 \pi b^3 V} \tag{6}$$

For all the above equations,

σ_a	is apparent conductivity in mhos/meter
I	is current in amperes
V	is induced potential in volts
a, b, c	are electrode spacings in meters (Figure 1), $b \geq 10a$ or $10c$ for Dipole and Schlumberger.
θ, β	are angles in degrees (Figure 1)

Some of the differences and advantages of the various arrays are evident from Figure 1 and equations (1) through (6). The Wenner array requires more wire for a given array size but has the greatest sensitivity, i.e., I/V is relatively small. The dipole arrays require the least wire and are least restricted in terminal locations. They are, however, relatively insensitive requiring large current sources and refined detection techniques. For a layered section, measured with comparable spacings, the Schlumberger array can locate boundaries twice as deep as an inline dipole array. A broadside dipole array can probe to the same depth as the Schlu nberger array, but is sensitive to lateral conductivity changes.

The sensitivity of dipole arrays to lateral conductivity changes can be greatly utilized by cross dipole measurements (see Appendix A). This

method involves two sets of current dipoles oriented at right angles to each other. Potential measurements are then made along the principal axes of another cross dipole. In other words, data is taken from an inline array and then from a broadside array at the same location. The interpretive advantage lies in the conductivity ratios formed from the pairs of measurements at common locations. These ratios, plotted vs. distance b, permits interpretation of lateral as well as vertical conductivity changes.

A difference not immediately evident from the electrode configurations and equations is the difference in maximum useable frequency. As mentioned above, the equations have been developed on the assumption of d-c currents and fields. The frequencies and spacings used, therefore must always be such that the spacings are not large compared to a skin depth in the earth at the frequency being used. In addition, the conductive coupling through the earth must be large compared to inductive and capacitive coupling between the connecting wires. Since the Wenner and Schlumberger arrays have current and potential leads closely paralleled, they are more restricted as to maximum useable frequency. Wait and Conda [1958] discuss these frequency limitations in more detail.

Effective depth of penetration or sounding depth becomes important when dealing with a layered earth. The discussion will be limited to the Eltran and dipole arrays since these are the arrays used in subsequent surveys. Wait and Conda [1958] and Keller [1965] have both investigated sounding for a two-layer earth in considerable detail. The results of their work are expressions for the ratio of apparent conductivity to first (or upper) layer conductivity as given below:

ELTRAN

$$\frac{\sigma_a}{\sigma_1} = \left\{ 3 \sum_{n=o}^{\infty} \epsilon_n k^n \left\{ \left[1 + (2nah/a)^2 \right]^{-1/2} + \left[9 + (2nah/a)^2 \right]^{-1/2} - 2 \left[4 + (2nah/a)^2 \right]^{-1/2} \right\} \right\}^{-1} \qquad (7)$$

$$\epsilon_o = 1, \quad \epsilon_n = 2 (n \neq o)$$

IN LINE (POLAR) DIPOLE

$$\frac{\sigma_a}{\sigma_1} = \left\{ 1 - \sum_{n=1}^{\infty} k^n \left\{ \left[1 + (2nah/b)^2 \right]^{-3/2} + 3 \left[1 + (2nah/b)^2 \right]^{-5/2} \right\} \right\}^{-1} \qquad (8)$$

EQUATORIAL (BROADSIDE) DIPOLE

$$\frac{\sigma_a}{\sigma_1} = \left[1 + 2 \sum_{n=1}^{\infty} k^n \left[1 + \left(\frac{2nah}{b} \right)^2 \right]^{-3/2} \right]^{-1} \qquad (9)$$

where for equations (7), (8), and (9)

σ_1 is the conductivity of layer one in mhos/meter,

k is the reflection coefficient, defined by $\frac{\sigma_1 - \sigma_2}{\sigma_1 + \sigma_2}$

n = 1, 2, 3 ----,

$a = \left|\frac{\text{conductivity in horizontal direction}}{\text{conductivity in vertical direction}}\right|^{1/2}$ or is the coefficient of anisotropy and is assumed = 1

h = thickness of layer one

and the earth is assumed to be uniform and isotropic. Equations (1, 2 and 7) are from Wait and Conda [1958]; equations (3, 4, 5, 6 and 8) are from Keller and Frischknecht [1965]; and equation (9) was computed from Wait and Conda [1958].

Theoretical curves for a two-layered earth can be plotted from equations (7, 8, and 9). These curves are dimensionless bi-logarithmic plots in which the ordinate is σ_a/σ_1. The abscissa term will vary depending on the array and a. a is usually assumed to be 1, unless data is available indicating otherwise. For the various dipole arrays, the abscissa term varies from b/h for the equatorial dipole to b/2h for the polar dipole. This variation shifts the curve horizontally. A complete family of curves is usually plotted with the ratio σ_a/σ_1 as a parameter. A family of such curves is shown in Appendix A, Figure A4. Sets of these curves are used for data interpretation by curve matching techniques.

Theoretical cross dipole curves are also plotted on bilogarithmic paper with the ratio of $\sigma_a/2$ inline to σ_a broadside as ordinate and the ratio of actual b spacing to layer thickness as abscissa. A theoretical set of such curves is shown in Appendix A, Figure A7 for a two-layer case, and Figure A 10 for a particular three-layer case.

It should be noted that the conductivity obtained with the above methods is the magnitude of the complex conductivity,

$$|\bar{\sigma}| = \sqrt{\sigma^2 + (\omega\epsilon)^2} \quad . \qquad (10)$$

For most survey work, $\omega\epsilon << \sigma$ so that the σ measured is the real part of the complex conductivity.

Data Interpretation

Field data is usually presented in a graphical log-log plot of apparent conductivity (σ_a) as some function of electrode spacing (b). If the dipole array is nearly a broadside, ($\theta = 90° \pm 15°$, $\beta = 90° \pm 15°$) equation (A 2), see Appendix A, is used to obtain the spacing factor. Similarly, if the array is nearly inline ($\theta = 0$, $\beta = \pm 15°$) equation (A 3) is used. If b' from equation (A 3) is divided by 2, then the data from an inline array and a broadside array can be plotted on the same data sheet and the spacing factor is the approximate depth of investigation.

Once the logarithmic field curves of σ_a vs. b' (spacing factor) are prepared, they are separated according to curve shape. Curve shape can indicate the number of layers, the sequence of layer conductivity, or some type of lateral conductivity change. After thus categorizing the curves, one may use various interpretation methods. A rather simple method is the curve matching technique. This technique generally yields layer conductivities σ_1, σ_2, and σ_3 for two and three layer earths as well as layer thickness h_1 h_2. Under certain conditions it may be impossible to determine a good value for anything other than the top layer conductivity and thickness. In such cases it is often possible to determine maximum or minimum on σ_2, σ_3 and h_2. h_2 and σ_2 are very often so related that their product is a constant;

thus if h_2 is high σ_2 will be low, and vice versa. Keller (see Appendix A, also [1965]), discusses the various interpretation techniques and their limitations in detail so no further discussion will be given here.

3. DECO FIELD OPERATIONS

3.1 Field Procedures

Survey sites are usually chosen because of some specific interest. Such interest may be a detailed survey over a small area or maximum coverage over a large area. Field procedures will vary somewhat for examples mentioned. The purpose behind the survey will dictate what survey methods and instrumentation will be used.

Detailed conductivity information is necessary, for example, for proper design of VLF and LF antenna systems. Such a survey can be limited to a small surface area and several hundred meters in depth because of the frequencies of interest (3 kc to 300 kc). Thus for this type survey, many shallow soundings are made. These soundings can be made solely with instrumentation described in Section 3.3.

In contrast, however, if the purpose of the survey is to examine and define the conductivity of geologic formations to great depths other procedures and instrumentation are used. First, a current site is chosen. The choice depends on geology of the surface and accessibility of roads surrounding the site to allow dipole and cross dipole measurements in four major directions from this current dipole site. A shallow sounding as mentioned above is made with the Eltran array to spacings of a = 500 m. Then the Dipole array is used with dipole lengths (a, c) of 500 m and dipole separations of b = 1 km to the limit of several tens of kilometers. The maximum spacing is limited by current input and the earth conductivity. Cross dipole measurements are made in areas where the road density will allow the dipoles to be laid out quickly and easily. Finally shallow soundings are made at or near the location of the potential dipole of the maximum spacings.

3.2 Instrumentation Used

Two systems are used; an audio-frequency transmitter and detector suitable for apparent conductivity measurements to depths of 5 km, and an ultra-low frequency synchronous detection system (deep probe) for measurements down to several tens of kilometers.

3.3 Audio System

The audio transmitter system consists of a vacuum tube power amplifier, with an input signal (20 - 20,000 cps) generated by an audio oscillator. An ac vacuum tube voltmeter measures the voltage drop across a precision 1 ohm resistor placed in series with the amplifier output and the current dipole stakes. It is, in effect, a current meter.

The wave analyzer used for a detector has a tuning range of 20 - 50,000 cps with a constant 3 db bandwidth of 7 cps. Maximum sensitivity is 30 μv full scale. Signal substitution calibration techniques are unnecessary, because the over-all gain and calibrated attenuators are accurate and stable. A block diagram of the system is shown in Figure 2.

3.4 Deep Probe System

The ultra-low frequency system is designed to operate at 0.625 cps, in order to avoid skin-depth effects. A block diagram of the system is shown in Figure 3. It is also designed to keep transmitter size, and consequently power, at a minimum. The receiver is designed to have a full scale sensitivity of 1 μv which is sufficient to detect a signal under the following conditions:

Dipole Array- - - - - - - - - - - - - a = c = 1 km, b = 60 km

Transmitter Current- - - - - - - - 1 ampere

Apparent Conductivity - - - - - - - 10^{-3} mhos/meter or less.

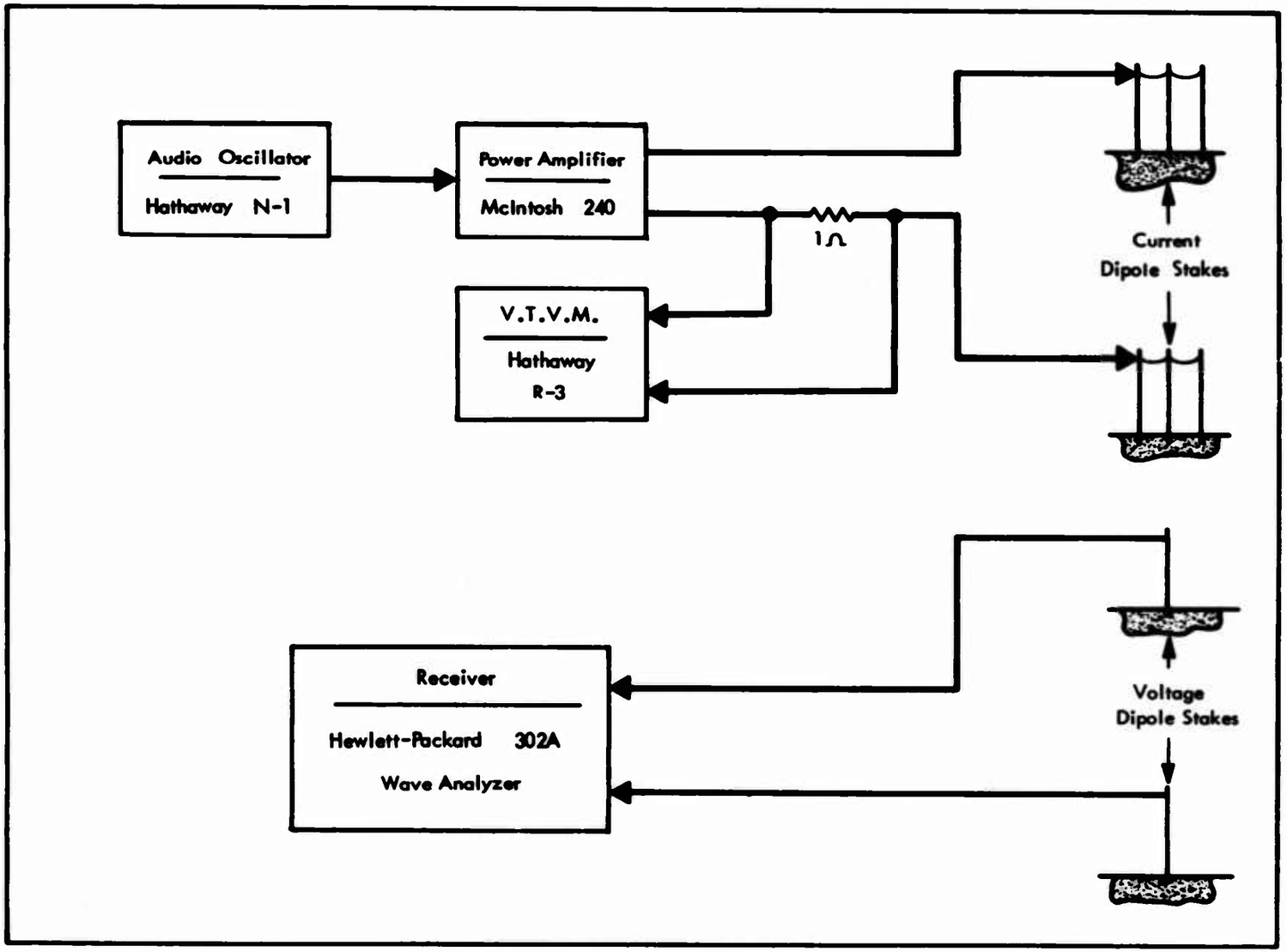

Figure 2 Audio Sounding Equipment

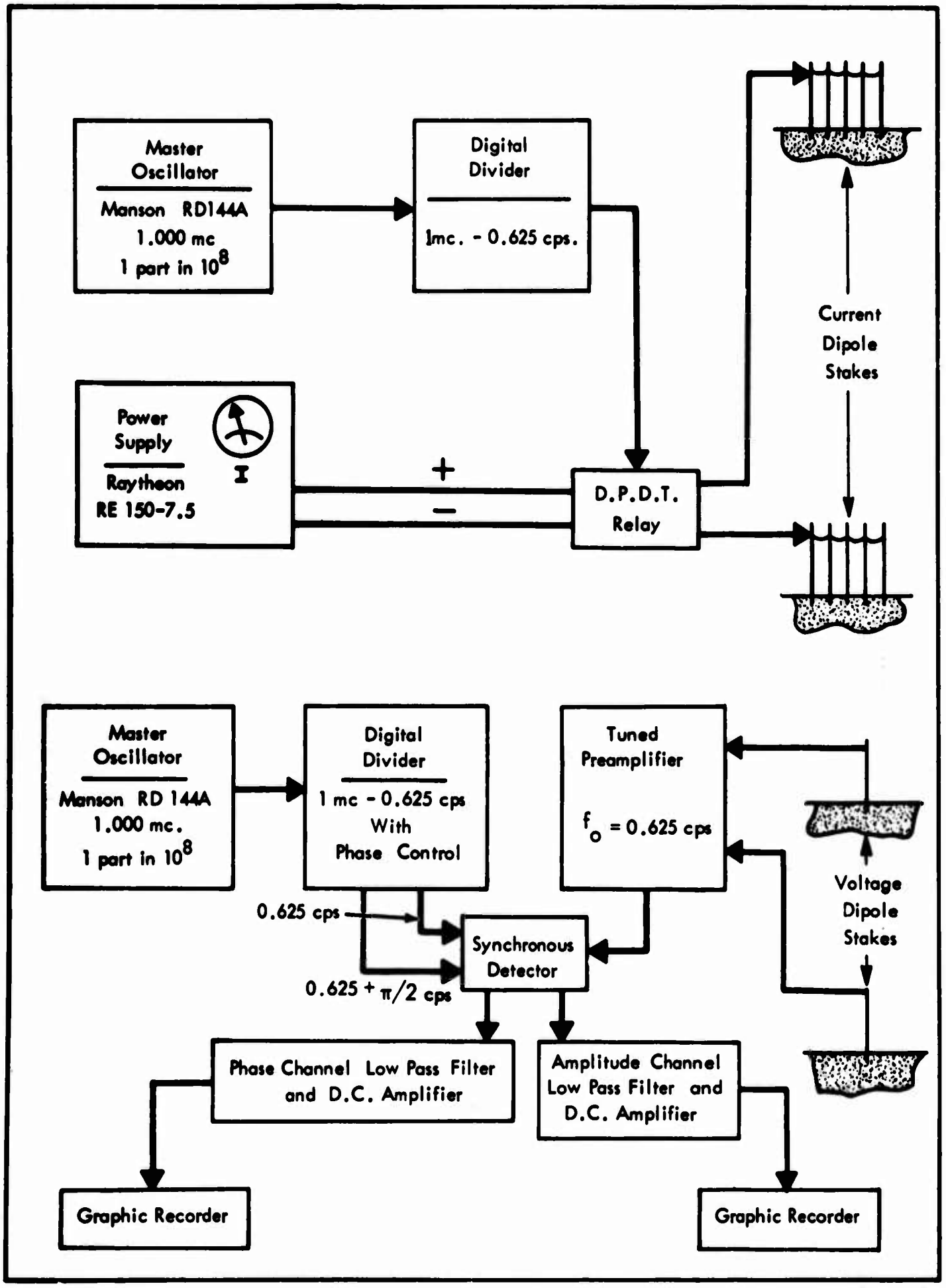

Figure 3 Deep Probe Equipment

The bandwidth required for this hypothetical system is determined by the natural telluric noise intensities. These vary considerably with location, season, diurnal and solar activity, but at this frequency a typical value would be 100 $\mu v/km/\sqrt{cps}$. For a S/N ratio of 0 db the detector bandwidth must be 10^{-4} cps. This bandwidth is achieved with the aid of synchronous (or correlation) detection, a detection scheme which modulates the received signal in synchronization with the transmitter frequency. The principle product cf this modulation has a frequency of zero which can be separated from unwanted signals and noise by low-pass R-C filters. A filter having a bandwidth of 10^{-4} cps requires 6360 seconds to respond to 98 percent of maximum for a step function input. To maintain synchronization within ± 3 percent for 6360 seconds the timing signals must be stable within 1 part in 10^6. This is exceeded by the 1.000 mc oscillator used which had a stability of 1 part in 10^8.

The oscillator output is divided down to 0.625 cps by five decade and four binary multivibrator circuits. The output of the final multivibrator controls a relay in the transmitter which commutates the output of a d. c. power supply into the ground stakes at each end of the current dipole. The current injected into the ground is measured with a series ammeter.

The receiver is made up of four main parts; (1) the tuned pre-amplifier and detectors, (2) the synchronization circuits, (3) the post detection filters and amplifiers, and (4) the graphic recorders.

Two different preamplifiers are used. The first type consists of two stages of operational amplifiers tuned by twin-T null circuits in their feedback loops. Maximum gain of this preamplifier is 80 db with a later addition of 20 db. The 3 db bandwidth at 0.625 cps is 0.05 cps. Calibrated attenuators control the gain.

The second preamplifier is made up of three operational amplifiers, each with a 30 db gain. They are coupled by band pass R-C filters and 0 to

30 db attenuators (10 db per step). The over-all low-pass cutoff (3 db) is at 0.1 cps and high-pass cutoff is at 3.4 cps for narrowband and 31 for wideband. The narrow bandwidths served to improve the signal-to-noise ratio ahead of the detectors and prevent overload.

Except for some added control functions, the synchronization oscillator and dividers of the receiver are identical to those of the transmitter. There are, however, two outputs in quadrature at 0.625 cps instead of one. These drive two single-pole, single-throw mercury relays which commutate or detect the preamp output. The detected quadrature outputs provide a phase and an amplitude record of the signal. The phase record serves primarily as an indication of synchronization.

Both detector outputs feed into variable R-C low-pass filters. D.C. operational amplifiers match the high impedance output of the R-C filters to the low impedance of Esterline-Angus graphic recorders which make permanent visual records of the measurement.

Two modes of operation are used. One, the synchronous mode, results in d. c. outputs proportional to the signal amplitude, $\cos\phi$ and $\sin\phi$ where ϕ is the relative phase between the signal transmitter and the receiver synchronization signal. For the rotating phase mode, the receiver synchronization frequency is offset from the transmitter frequency such that the detected output is the difference frequency of an amplitude proportional to the signal. This difference frequency is adjusted to fall close to the low-pass filter cutoff frequency. Figures 4a and 4b show a pair of representative records which were made in the completely synchronous mode. They show that the amplitude channel output rises to a maximum in four time-constants of the output R-C filter, while the phase channel stays around zero. The maximum output level is referred to the receiver input voltage by signal substitution

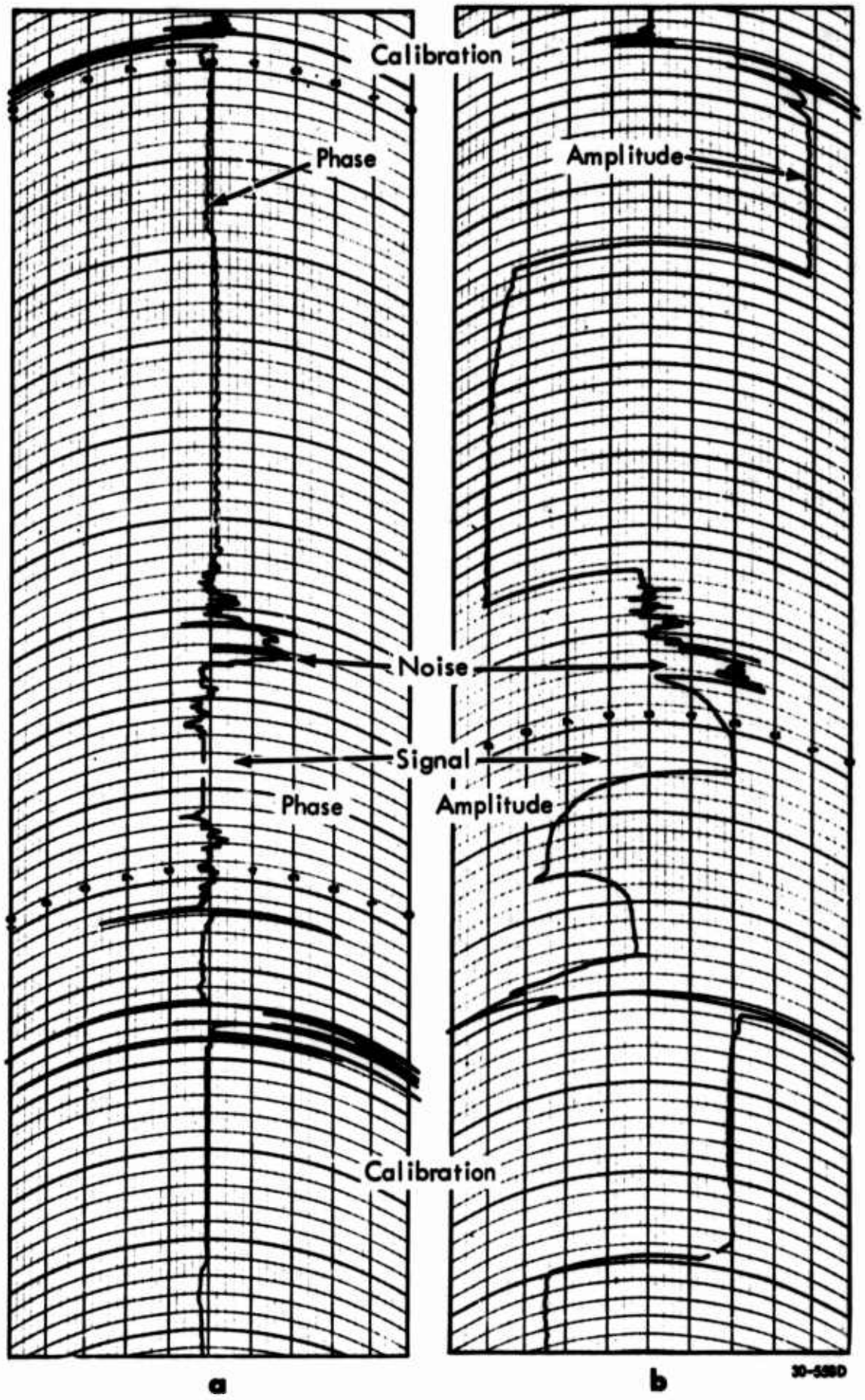

Figure 4,a,b Sample of Synchronous Mode 1 Deep Probe Records

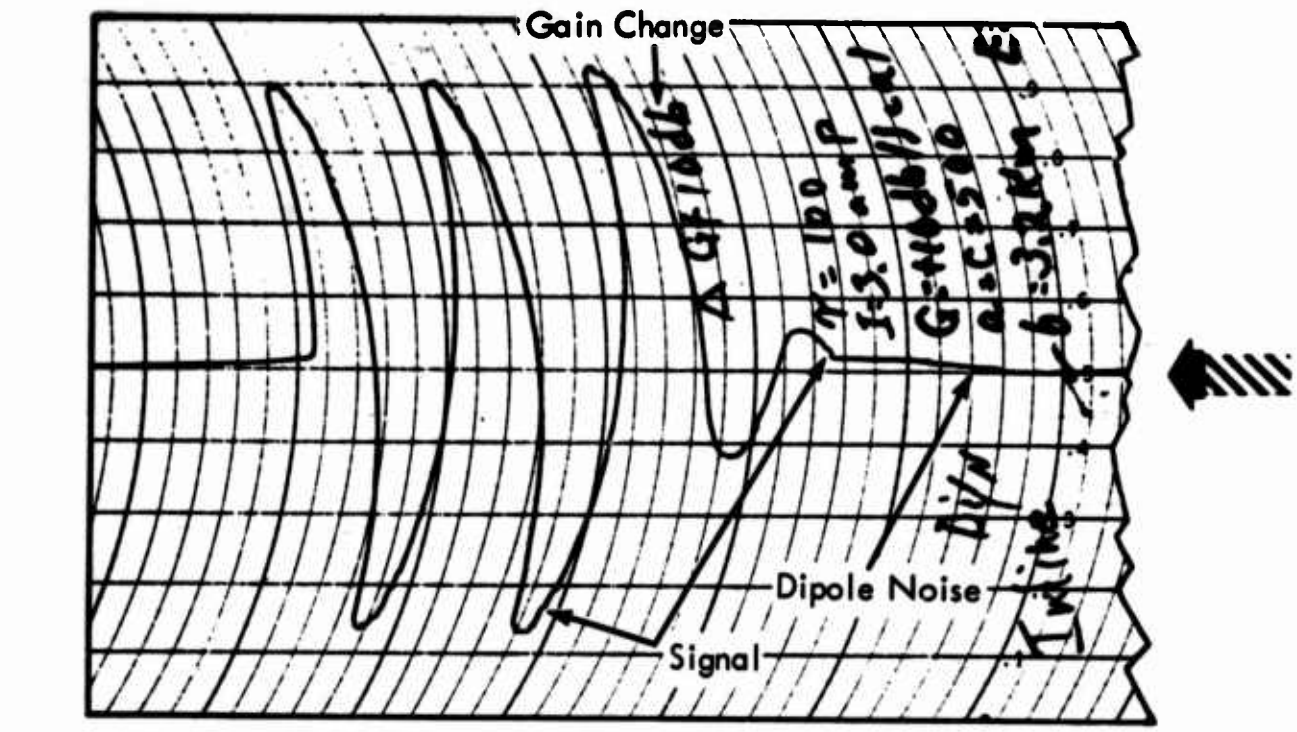

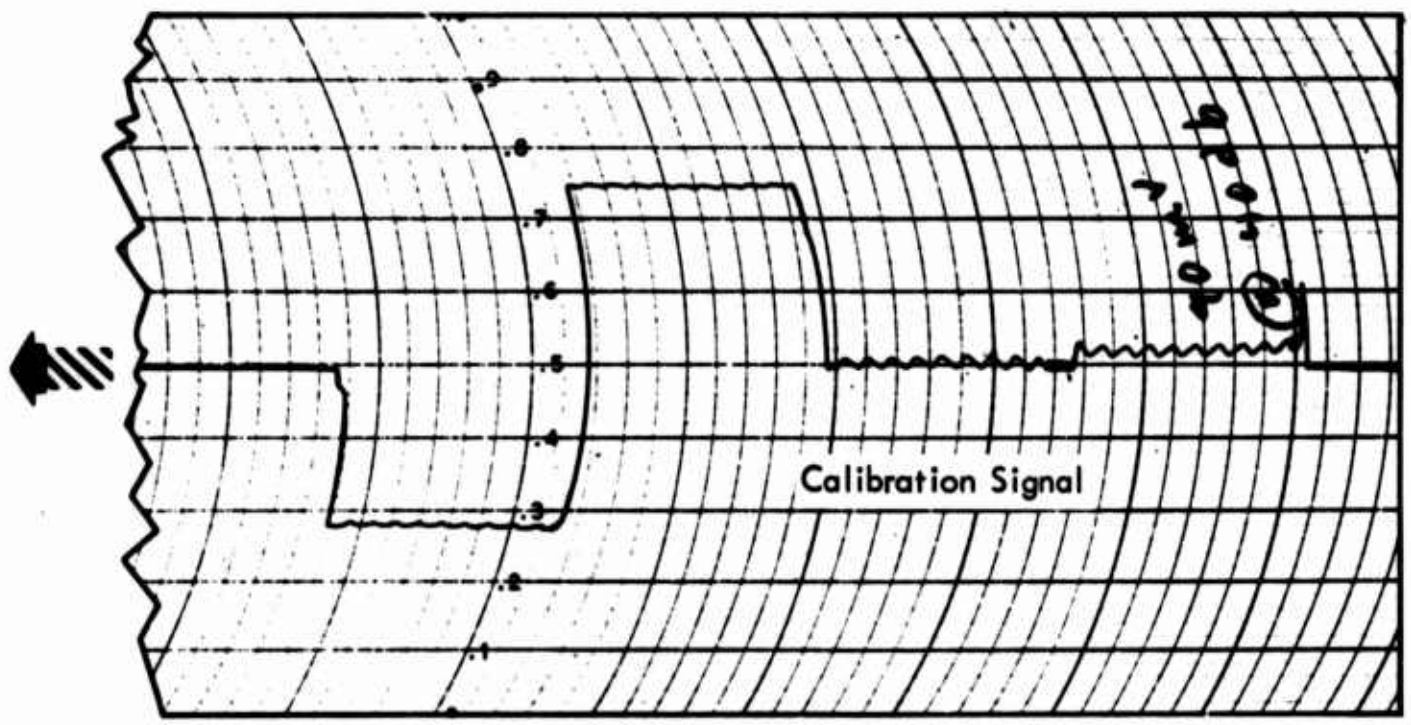

30-586D

Figure 4c (Cont.) Sample of Rotating Phase Deep Probe Records

calibration. The record in Figure 4c was made using a rotating phase mode in which the frequency of the receiver's modulator signal generator is slightly offset from that of the transmitter. The frequency difference is recorded and its peak to peak amplitude is referenced to the input by signal substitution calibration.

4. CONCLUSIONS

This report is a tutorial report covering the theory, field methods, instrumentation and interpretation as used by DECO in geoelectric surveying. As procedures and instrumentation are improved, they will be covered in future reports. Therefore, this report should be correlated with present and future DECO 30 conductivity survey reports.

5. REFERENCES

Fine, H., (1954), An effective ground conductivity map for Continental United States, Proc. IRE, Vol. 42, No. 9, p. 1405.

Keller, G.V., and F.C. Frischknecht, (1965), Electrical methods in geophysical prospecting, (Pergamon Press).

Morgan, R.R., and E.L. Maxwell, (1965), Omega navigational system conductivity map, DECO Report 54-F-1, January 1963, Contract NOnr 4107(00), Nr 371-630.

Wait, J.R., and A.M. Conda, (1958), On the measurement of ground conductivity at VLF, IRE Transactions on Antennas and Propagation, Vol. AP-6, No. 3, July.

Watt, A.D., and E.L. Maxwell, (1960), Measured electrical properties of snow and glacial ice, NBS Jour. of Res., Vol. 64D, No. 4, July - Aug.

Watt, A.D., F.S. Mathews, and E.L. Maxwell, (1962), Some electrical properties of the earth's crust, Proc. IEEE, June, also DECO Report 30-S-1, submitted to U.S. Navy Dept., on Contract NOnr 3387(00), 7 March 1962.

APPENDIX A

MANUAL FOR THE INTERPRETATION OF LAYERED CONDUCTIVITY CURVES FOR THE SEQUENCE HIGH-LOW-HIGH

By

Dr. G. V. Keller

FIGURES

Figure		Page
A 1	Inline and broadside dipole arrays.	A-13
A 2	Non-ideal dipole array.	A-13
A 3	Effective spacing factor for non-ideal dipole array.	A-14
A 4	Theoretical curves for the broadside array over a single overburden resistive basement.	A-15
A 5	Theoretical curves for the inline array over a single overburden resistive basement.	A-16
A 6	Crossed dipole array.	A-17
A 7	Ratio curves for single overburden.	A-18
A 8	Broadside array, 1:1/4:1	A-19
A 9	Inline array, 1:1/4:1	A-20
A 10	Crossed dipole ratio, 1:1/4:1	A-21
A 11	Broadside array, 1:1/4:∞	A-22
A 12	Inline array, 1:1/4:∞	A-23
A 13	Broadside array, 1:1/39:1	A-24
A 14	Inline array, 1:1/39:1	A-25
A 15	Crossed dipole ratio, 1:1/39:1	A-26
A 16	Broadside array expanded in the dip direction over dipping insulator.	A-27
A 17	Inline array expanded in the dip direction over dipping insulator.	A-28
A 18	Crossed dipole ratio for receivers moving up dip over a dipping insulator.	A-29
A 19	Crossed dipole ratio for receivers moving downdip over a dipping insulator.	A-30
A 20	Broadside array expanded across a fault-like change in the conductivity of a surface layer covering an insulator.	A-31

Figure		Page
A 21	Inline array expanded across a fault-like change in the conductivity of a surface layer covering an insulator.	A-32
A 22	Crossed dipole ratio for receivers expanded across a fault-like change in the conductivity of a surface layer covering an insulator.	A-33
A 23	Broadside array expanded parallel to a fault-like change in the conductivity of a surface layer covering an insulator.	A-34
A 24	Inline array expanded parallel to a fault-like change in the conductivity of a surface layer covering an insulator.	A-35
A 25	Crossed dipole ratio for receivers expanded parallel to a fault-like change in the conductivity of a surface layer covering an insulator.	A-36
A 26	Broadside array curves for three layers H-L-H if the middle layer has a much lower conductivity than the other layers.	A-37
A 27	Inline array curves for three layers H-L-H if the middle layer has a much lower conductivity than the other layers.	A-38

APPENDIX A

MANUAL FOR THE INTERPRETATION OF LAYERED CONDUCTIVITY CURVES FOR THE SEQUENCE HIGH-LOW-HIGH

Dr. G. V. Keller

DEFINITION OF PROBLEM

The curves contained in this Appendix are compiled for the specific problem of interpreting apparent conductivity measurements made with ideal dipole arrays over a layered earth presumably consisting of a low-conductivity zone sandwiched between two more highly conductive zones. The problem in interpretation consists of two parts:

1. Determination that the apparent conductivity measurements represent a horizontally-layered earth and not an earth with lateral changes in the conductivity of a surface layer; and

2. Determination of the conductivities and depths of the layers, and particularly of the low-conductivity layer, once the data are determined to represent a layered earth.

For the most part, the interpretation curves are compiled for ideal dipole arrays, those arrays in which the sending and receiving dipoles are negligibly short in comparison with their separation. In most field applications, this requirement is satisfied if each dipole length is less than 1/5 the dipole separation. The interpretation curve sets are compiled only for two very special ideal dipole arrays--the broadside (equatorial) array and the inline (polar) array, as shown in Figure A-1. In the broadside array, the two dipoles are parallel to one another, and in making a sounding, the receiving dipole is

moved out along the equatorial axis of the sending dipole. In the inline array, the two dipoles are located along a common line, and in making a sounding, the receiver dipole is moved out along the polar axis of the sending dipole.

Usually these requirements are not met exactly in a field survey. Measurements are made with a completely general dipole array, in which the receiving dipole is located along a radius vector making an azimuth angle θ with the sending dipole axis, and with a bearing angle β between the radius vector and the axis of the receiving dipole (see Figure A-1). A value for the apparent conductivity of a uniform earth may be computed from the formula:

$$\sigma_a = \frac{I\,a\,c}{\pi\,b^3\,V}\left(\cos\theta\cos\beta + \frac{1}{2}\sin\theta\sin\beta\right) \quad \text{(A-1)}$$

where $\underline{b}$ is the separation between dipole centers and $\underline{a}$ and $\underline{c}$ are the lengths of the sending and receiving dipoles $\beta = |\theta - \phi|$. The term $\underline{b}$ is many times written as $\overline{OP}$.

The apparent conductivity values so determined may be compared with theoretical curves for broadside or inline arrays only if the azimuth angle is very close to 90° or 0°, respectively. For azimuth angles up to 15° different from these values, the theoretical curves may be used if a corrected dipole spacing $\underline{b'}$ is used rather than the actual separation between dipole centers, $\underline{b}$. If the angles θ and B are within 15° of being 90°, the curves for a broadside or Schlumberger array may be used if the dipole separation is defined as:

$$\underline{b'}\ (\text{Broadside}) = b\,\frac{\sin\theta + \cos\beta}{\sin\theta + 2\cos\beta} \quad \text{(A-2)}$$

where b is again the actual separation between dipole centers. If the angles θ and β are within 15° of being 0°, the curves for an inline array may be used if the dipole separation is defined as:

$$\frac{b'}{---}(\text{inline}) = 2b \quad \frac{\sin\theta + \cos\beta}{\sin\theta + 2\cos\beta} \qquad \text{(A3)}$$

The value of b' as defined in equation A-3 must be used with the usual theoretical inline dipole curves. If equation A-3 is divided by 2, the resulting inline data can be compared to theoretical broadside or Schlumberger arrays. Equations A-2 and A-3 can be extended beyond the ±15° limits, but for larger deviations of the azimuth angle, the probability of error becomes larger, particularly in the use of ratio curves (defined later).

The same approach - that of redefining the apparent dipole separation - may be used in considering measurements made close to the sending dipole, so that the approximation that dipole lengths are small cannot be made. With all four electrodes along a common line, and with the distances between electrodes specified as shown in Figure A-2, the corrected spacing factor should be

$$a' = r \; \frac{\ln\left[\left(1+\frac{c}{r}\right)\frac{1+\frac{a}{r}}{1+\frac{a}{r}+\frac{c}{r}}\right]}{1 - \frac{1}{1+\frac{c}{r}} - \frac{1}{1+\frac{a}{r}} + \frac{1}{1+\frac{a}{r}+\frac{c}{r}}} \qquad \text{(A-4)}$$

where r is the distance between near ends of the dipoles, rather than the distance between centers. Curves showing the variation in effective spacing factor as a function of actual electrode separations are given in Figure A-3. The apparent conductivity is calculated using the formula

$$\sigma_a = \frac{I}{2\pi V}\left(\frac{1}{AM} - \frac{1}{AN} - \frac{1}{BM} + \frac{1}{BN}\right) \qquad \text{(A-5)}$$

where I is the current to the ground and V is the measured voltage. Using the spacing factor and apparent conductivity computed in this way, data obtained close to one end of a sending dipole can be interpreted using the theoretical curves for a broadside array.

Single Overburden

Field observations are first interpreted using theoretical curves for a single, uniform overburden covering a homogeneous half-space which has a conductivity different than that of the overburden. If the half-space has a lower conductivity than the overburden, the observed conductivity will vary with dipole separations as indicated by the curves in Figures A-4 and A-5. The two sets of curves, those for the broadside array and those for the inline array, are generally similar in character but have one significant and important difference; the curves for the inline array will correspond closely with the curves for the broadside array only if the dipole separation for the inline array is halved. This indicates that to locate a buried insulator with the inline array requires the use of dipole separations twice as large as those which would be required if the broadside array were used.

The theoretical curves for the case in which the buried half-space is an insulator possess a characteristic which is useful in interpretation: the observed conductivity decreases linearly with increasing dipole separation if the dipole separation is more than twice the overburden thickness. When this linear decrease in observed conductivity with increasing spacing is observed, then for any pair of values (σ_a, b), the following relationships hold:

$$b\sigma_a = h_1\sigma_1 = S \qquad \text{(for a broadside array)} \qquad \text{(A-6)}$$

and

$$\frac{b\sigma_a}{2} = h_1\sigma_1 = S \qquad \text{(for an inline array)} \qquad \text{(A-7)}$$

The quantity, S, is called the conductance of the overburden, and is useful in interpretation.

If the conductivity of the lower half-space is not exactly zero, the observed conductivity values will depart progressively from this linear decrease relationship, until for very large dipole separations the observed conductivity closely approximates the actual conductivity of the lower half-space. The conductivity of the lower half-space may be estimated by comparing the observed conductivities with these theoretical curves.

If the conductivity of the lower half-space is a very small fraction of the overburden conductivity, the deviation of the observed values from the linear decrease relationship may be emphasized if the observed values are multiplied by the dipole spacing. The advantage of this form of data presentation lies in the possibility of expanding the vertical scale on the data plots and on the theoretical curves to emphasize the departure from a linear decrease relationship. Spacing-multiplied theoretical curves with the vertical dimension increased by factors of two and five are available.

In using such curves, the observed data must be plotted on a special bi-logarithmic graph paper in which the decades are stretched vertically by the ratios indicated on the spacing-corrected theoretical curves. The better the precision of the data, the greater can be the vertical stretching ratio which is applied. However, it appears not to be possible to distinguish between these effects and the effect of a non-zero conductivity in a half-space if data obtained with only one type electrode array are available.

One method of obtaining enough data to separate these various effects is by the use of a crossed dipole current source, so that broadside and inline measurements may be made at the same points along a common traverse (see Figure A6). Measurements made in this manner provide an additional set of curves which is useful in interpretation; the ratio of inline apparent conductivity to broadside apparent conductivity for a common dipole separation. For the single overburden problem, this ratio varies at most by a factor of two, as indicated by the curves in Figure A-7. This behavior of the ratio will be useful when considered in comparison with the behavior of the same ratio in

cases where conductive layers are present at depth or in cases where there are lateral changes in the conductivity of a surface layer.

THREE LAYERS

Curves resembling those for the single overburden problem may be obtained in an earth consisting of three layers, with the top layer and the lower layer (taken to be a uniform half-space) having a higher conductivity than the middle layer. This ambiguity may be resolved by using dipole separations great enough to detect the conductivity of the third layer, but commonly, it is not practical to use such large separations. If so, the third layer will cause the observed conductivities to deviate from an inverse linear relationship in a way very similar to the effect caused by a non-zero second-layer conductivity, and the conductivity of the second layer will be assigned too large a value.

Curves for the three-layer problem may be constructed as a function of three parameters; the ratio of second-layer conductivity to first-layer conductivity, σ_2/σ_1; the ratio of third-layer conductivity to first-layer conductivity, σ_3/σ_1, and the ratio of second-layer thickness to first-layer thickness, h_2/h_1. A family of curves for the three-layer case here is taken as a set of curves for a group of values for the parameter h_2/h_1, and single values for the parameters σ_2/σ_1 and σ_3/σ_1. Curves are available for 10 values of the parameter h_2/h_1, ranging from 1/9 to 24. For lesser ratios, the effect of the layer can largely be ignored, while for larger ratios, usually the observed conductivities can be treated in two parts, each part of the data corresponding reasonably well to a single-overburden problem.

The following families of curves are included in this album:

Figure	Array	σ_2/σ_1	σ_3/σ_1
A8	Broadside	0.25	1.0
A9	Inline	0.25	1.0
A10	Crossed ratio	0.25	1.0
A11	Broadside	0.25	∞
A12	Inline	0.25	∞
A13	Broadside	0.0526	1.0
A14	Inline	0.0526	1.0
A15	Crossed ratio	0.0526	1.0

This manual contains only the minimum number of curves to discuss the problems involved. Many more curves are available and can be computed for many other parameters.

Several features of these curve sets should be recognized in interpretation. Interpretation problems for which these three-layer curves are useful may be of two types:

1. Problems in which dipole separations were not large enough for the observed conductivities to follow the theoretical curves through a minimum. In such problems, it is necessary to distinguish the data from a single-overburd case before three-layer interpretation curves can be used.

2. Problems in which dipole separations were large enough for the observed conductivities to follow the theoretical curves through a minimum. In such problems, three-layer interpretation curves may be used, but consideration must subsequently be given to the possibility that the observed minimum may be caused by lateral changes in the conductivity of the overburden rather than by the presence of a conductive bed at depth.

In the first problem, if the data are sufficiently precise, it is possible to detect the presence of the conductive third layer by the effect it has on the ratio of resistivities measured along a common profile about a crossed dipole source. For the case of a single overburden (Figure A 7), the ratio varies from 1/2 to 1 and back to 1/2 as the dipole separation is increased, being asymptotic to the value 1/2 from above at very large separations. In the three layer problem, the ratio also goes through a maximum, but then decreases to values less than 1/2, corresponding to spacings past the minimum on the apparen conductivity curves. The ratio passes through a value of 1/2 at the spacing at which ne minimum conductivity is measured with the broadside array. Therefore, the first segment of a three-layer curve can be distinguished from the corresponding single-overburden curve which would provide the best fit to the same data by providing ratio values about 10 to 30 percent lower than those for that single overburden interpretation.

LATERAL EFFECTS

The behavior of the ratio curves provides a much more powerful tool for the solution of the second problem mentioned above--distinguishing between a third, conductive layer at depth and a lateral change in the conductivity of the overburden. Curves are included only for a few special types of lateral changes, inasmuch as if they exist and can be recognized, it is sufficient to discard the data. There is no interest in interpreting the character of a lateral change in the overburden in detail, since this interpretation will not provide information about rocks at depth.

Two special types of problems may be considered; the effect of a dipping contact between zones with different conductivity on the conductivity values observed at the earth's surface, and the effect of a change in the conductivity of a surface layer covering an insulating half-space. In each of these two types of problems, only measurements made with arrays expanded exactly normal to or exactly parallel to the strike of the conductivity structure will be considered; conductivities measured with arrays oriented otherwise may be inferred.

Curves for arrays expanded updip or downdip over a dipping insulator are given in Figures A16 (for the broadside array) and A17 (for the inline array).

In three out of the four possible cases, the effect of dip is similar to the effect of a third conductive layer, in that the apparent conductivity determined at large dipole separations increases. Only for the case of a broadside dipole array with the receiver being moved updip, are the apparent conductivities diagnostic. In this case only, the apparent conductivity decreases more rapidly with increasing spacing than does the conductivity value measured over a flat-laying insulator. This behavior, (a decrease in conductivity which is more than proportional to the increase in spacing) is always indicative of the updip direction for a buried resistant bedrock.

In the other three cases - the broadside array with the receiver moving downdip, and the inline array with the receiver moving either updip or downdip -

values for the ratio of inline-to-broadside conductivities can be used to distinguish the effect of dip from the effect of a third conductive layer at depth. Ratio curves for receivers moving updip are given in Figure A18 and for receivers moving downdip, in Figure A19. In both cases, the ratio becomes very much greater than unity, though the increase is most pronounced in the updip direction.

No curves specifically computed for arrays expanded parallel to the strike are included here, since the effect is similar to that due to a lateral change in the conductivity of a surface layer.

Curves for dipole arrays expanded across a fault-like change in conductivity of a surface layer covering an insulating substratum are shown in Figures A20 (for the broadside array) and A21 (for the inline array). At first glance, the two sets of curves appear very similar. However, on expanding the receiver of a dipole array across a fault-like boundary, the measured conductivity changes in the opposite sense to that measured with an inline array under the same circumstances. If the receiver of a broadside array crosses into a more conductive zone, the observed conductivity suddenly increases. On the other hand, if the receiver of an inline array crosses into a conductive zone, the observed conductivity decreases.

This inverse behavior of the curves obtained with the two arrays leads to a wide range in values of the ratio, inline-to-broadside (see Figure A22). The ratio of observed conductivities, 1/2 - inline to broadside, exactly equals the resistivity ratio across the fault and is in the opposite sense. Although these curves don't show it, the ratio full-inline to broadside equals the resistivity ratio across the fault, also in the opposite sense if the insulating substratum is not present or is so deep that it does not affect the measurements.

Curves for the behavior of conductivity measurements made by expanding an array parallel to the same fault-like change in the conductivity of a surface layer covering an insulating substratum are given in Figures A23 (for the broadside array) and A24 for the inline array). For certain contrasts in

resistivity in the surface layer, these curves exhibit minimums which might be confused with the effect of a non-zero second-layer conductivity or with the presence of a third, conductive layer. With an inline array, the presence of a highly conductive bed parallel to the array enhances the value of observed conductivity, while the opposite is true for the broadside array. This leads to very large ranges in the value for the 1/2 - inline to broadside conductivity ratio, (see Figure A25). For dipole separations which are large compared to the offset distance of the array from the fault in the surface layer, this ratio becomes exactly equal to the ratio of resistivities across the fault and in the same sense. Again, though it is not shown by these curves, the ratio full-inline to broadside conductivity is exactly equal to the resistivity ratio across the fault, in the same sense, if the insulating substratum is not present or is so deep that it does not affect the measurements.

THREE-LAYER CURVES FOR LARGE CONDUCTIVITY CONTRASTS

In the sequence of conductivities High-Low-High, if the contrast in conductivity between adjacent layers becomes larger than 39, the three-lay curves contained in the first portion of this report are not adequate for inte pretation. Moreover, when conductivity contrasts are large, it is usually n possible to make an interpretation uniquely in terms of the conductivity of t second layer. Instead, it is possible to determine only a value for the ratio h_2/σ_2, the thickness of the low conductivity layer divided by its conductivity

Curves for interpreting conductivity measurements obtained with a broadside array under these conditions are given in Figure A26, and for the inline array, in Figure A27. These curves are normalized about their mini points. Conductivities may approach any finite value more than twice the m value along the appropriate single-overburden curve drawn tangent to this g curve. The minimum point on the curve gives the characteristics of the lov conductivity layer as follows:

$$h_2/\sigma_2 = b/\sigma_a \quad \text{(at minimum, for the broadside array)}$$

$$h_2/\sigma_2 = 1.2\, b/\sigma_a \quad \text{(at minimum, for the inline array).}$$

While the conductivity of the second layer cannot be specified, it must be le than $1/2\,\sigma_{min}$ for the broadside array, or less than $0.6\,\sigma_{min}$ for the inline array.

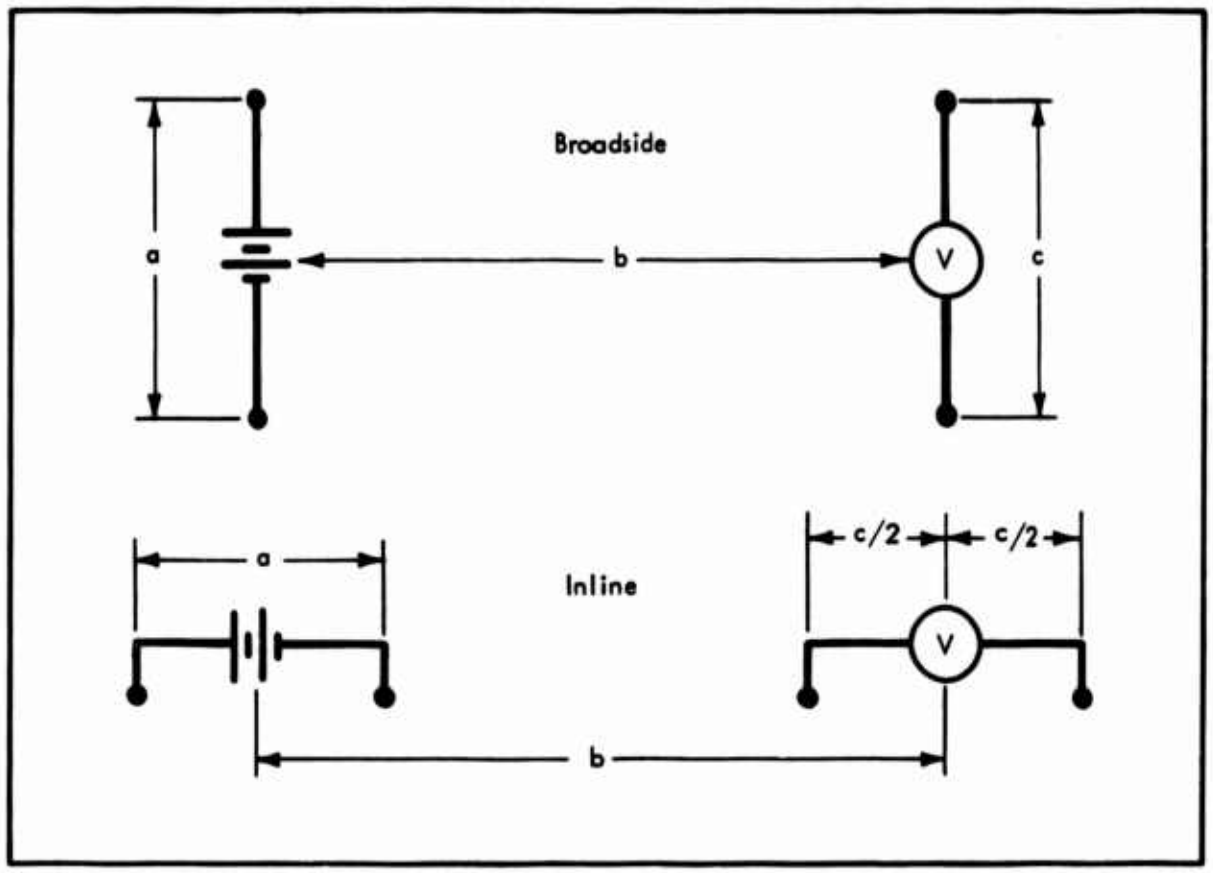

Figure A1 Inline and Broadside Dipole Arrays

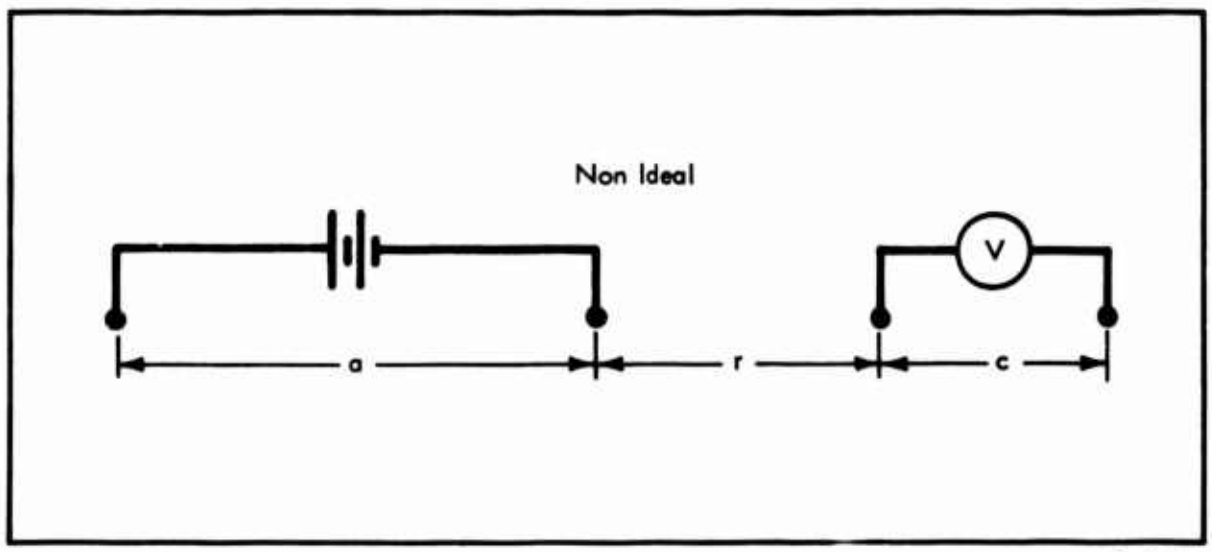

30-595D

Figure A2 Non-Ideal Dipole Array

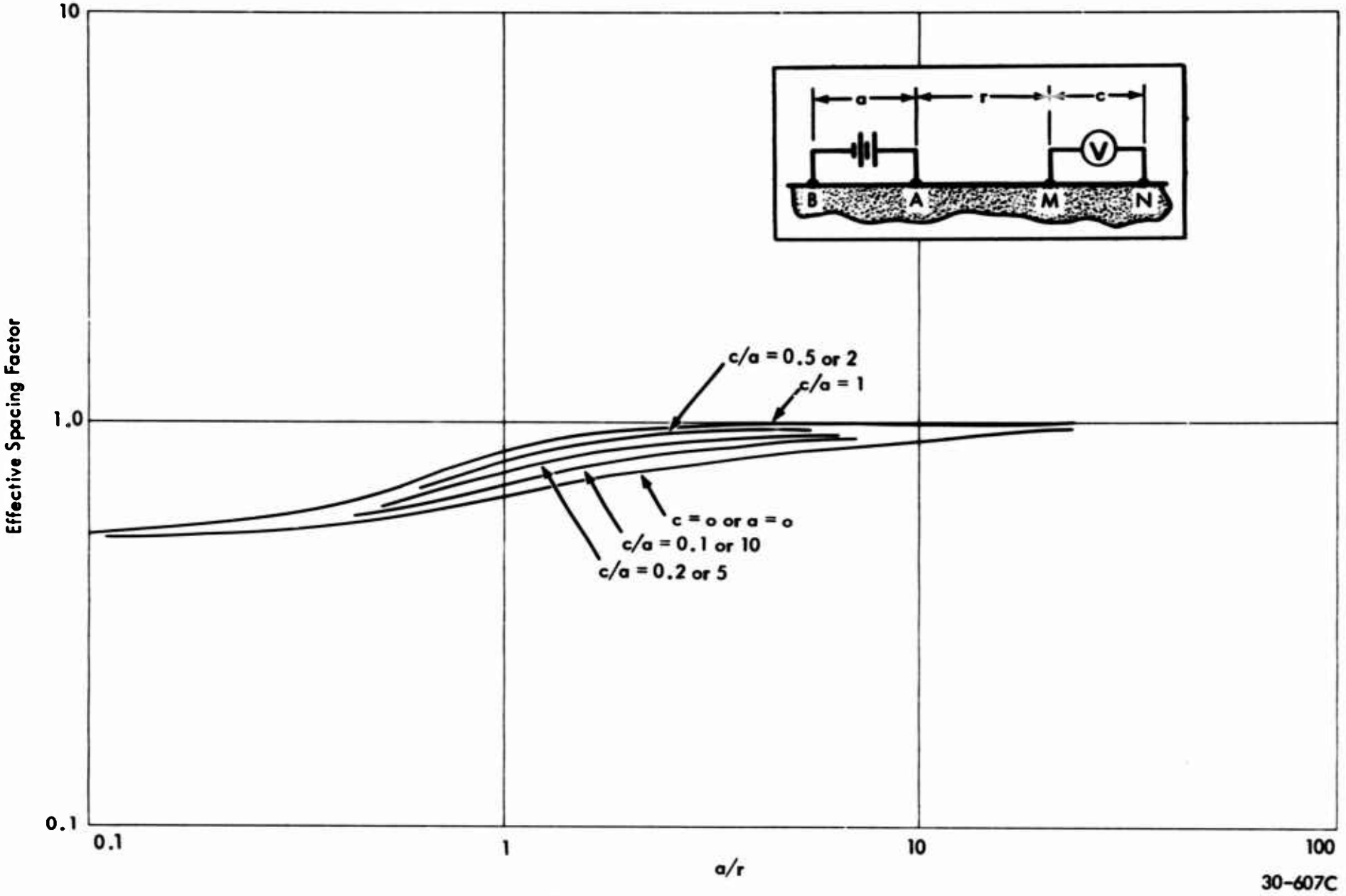

Figure A3 Effective Spacing Factor for Inline Array if Dipoles Both Cannot be Considered Short

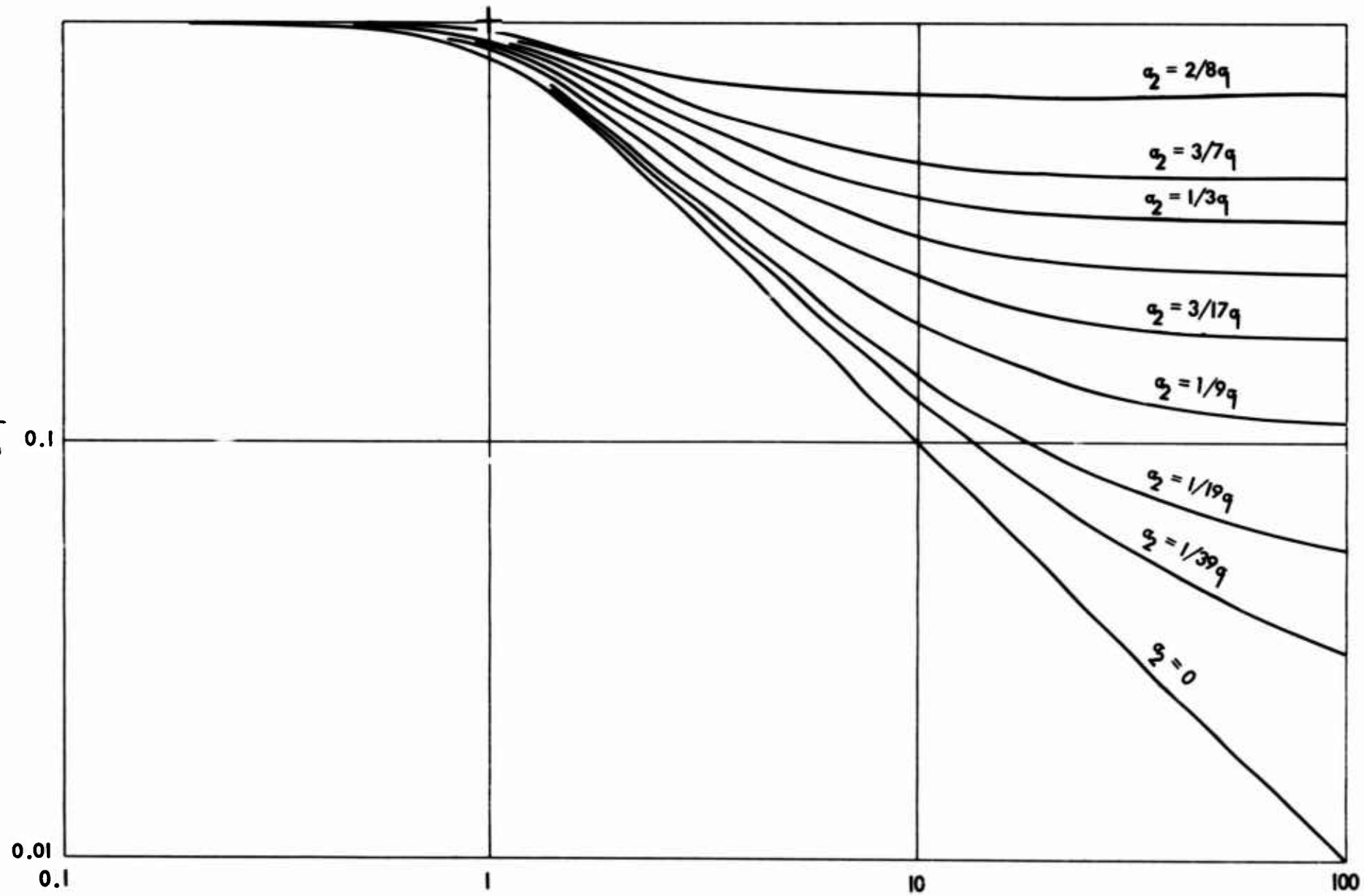

b Spacing/Layer Thickness

Figure A4 Broadside (Equatorial)

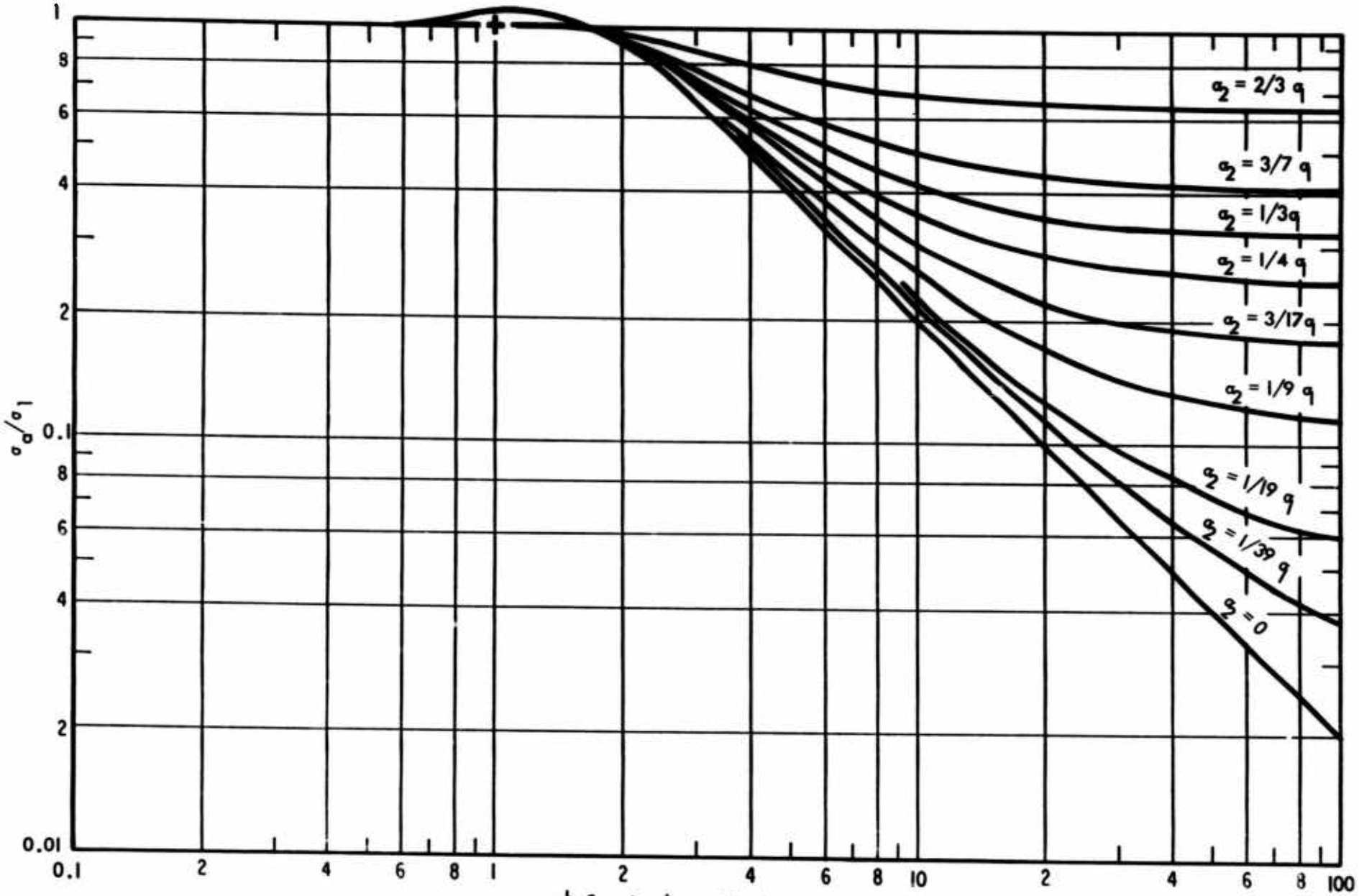

Figure A5 Inline (Polar)

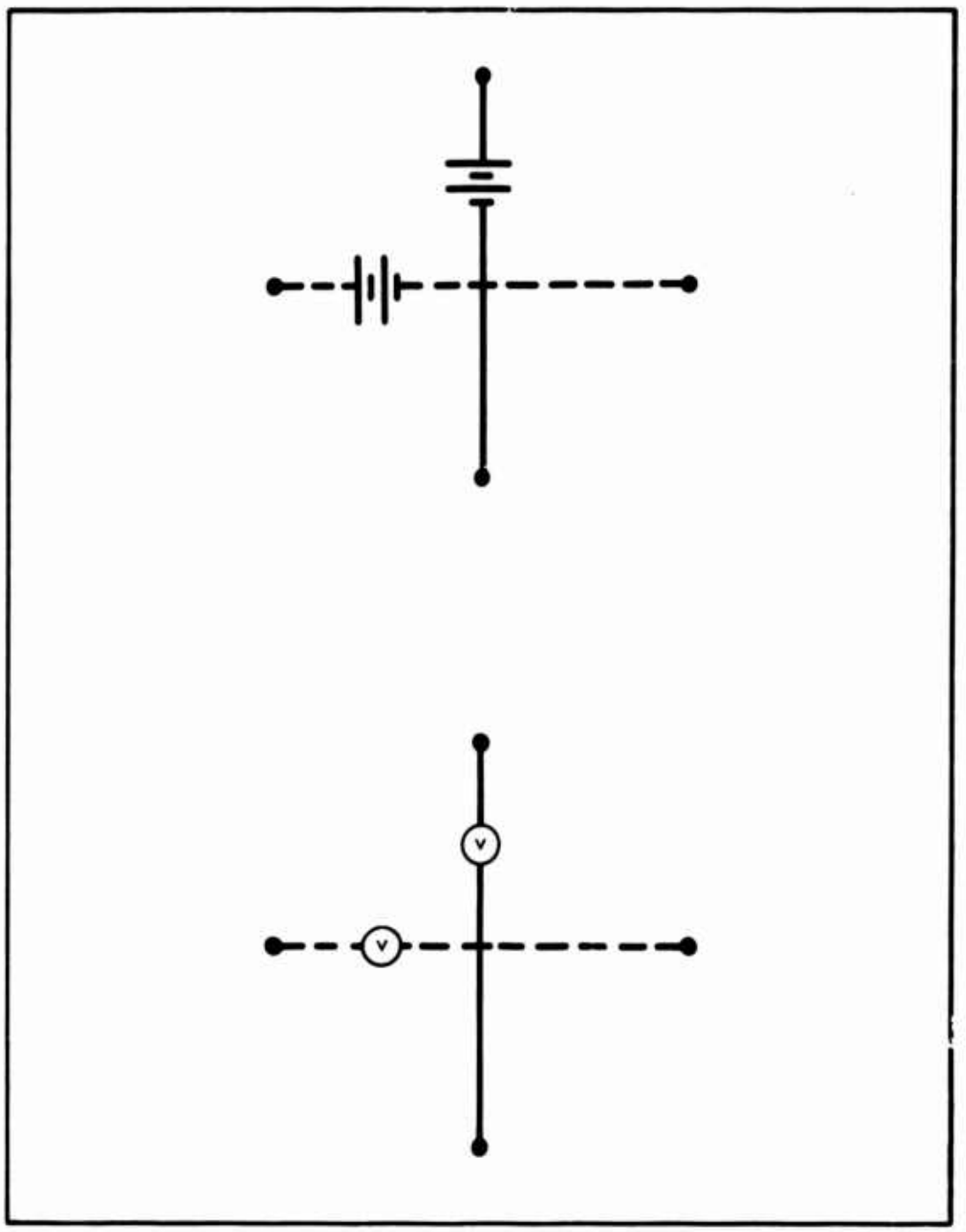

Figure A.6 Crossed Dipole Array

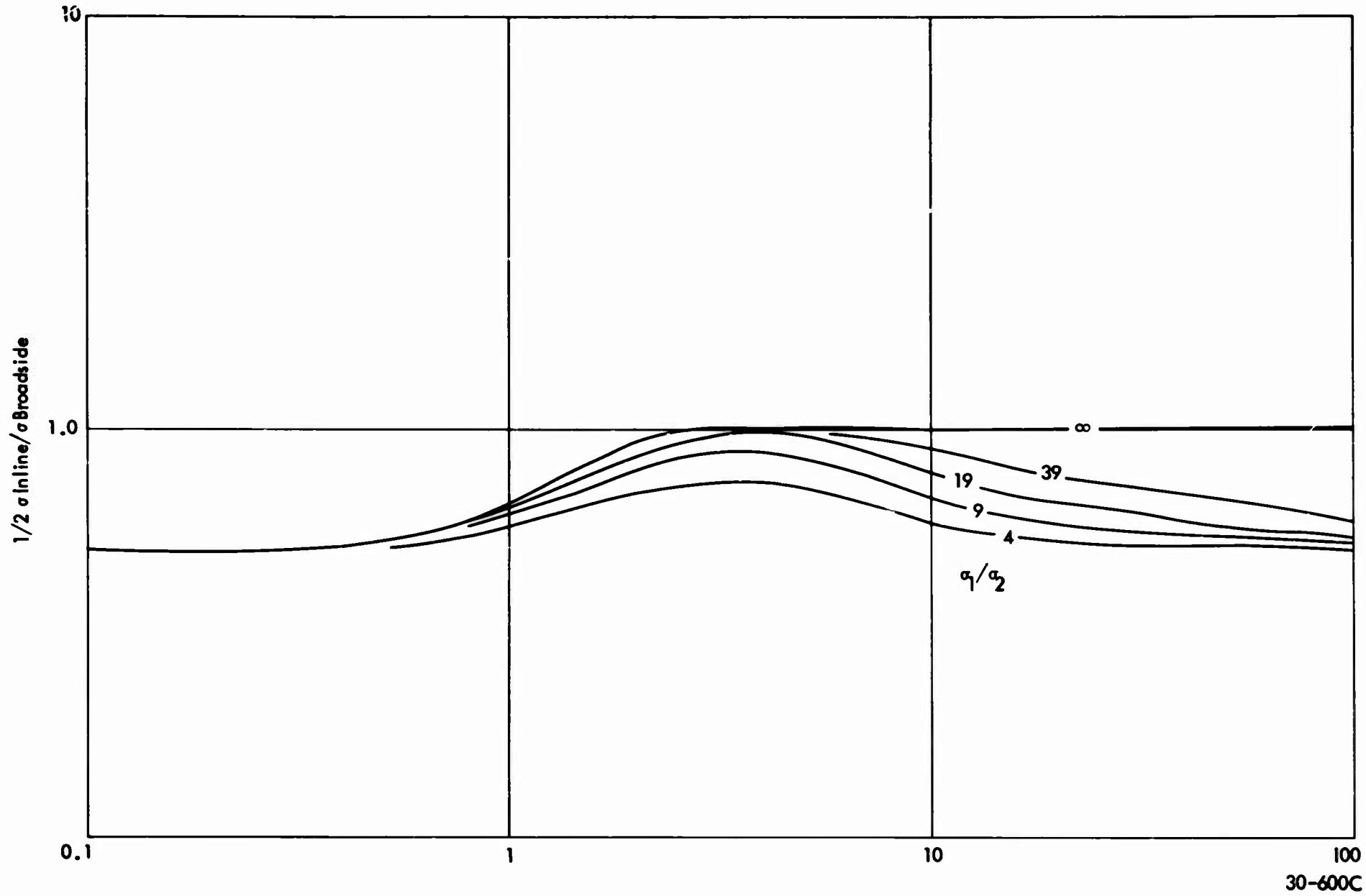

Figure A7 Single Overburden Radio of 1/2 Inline to Broadside

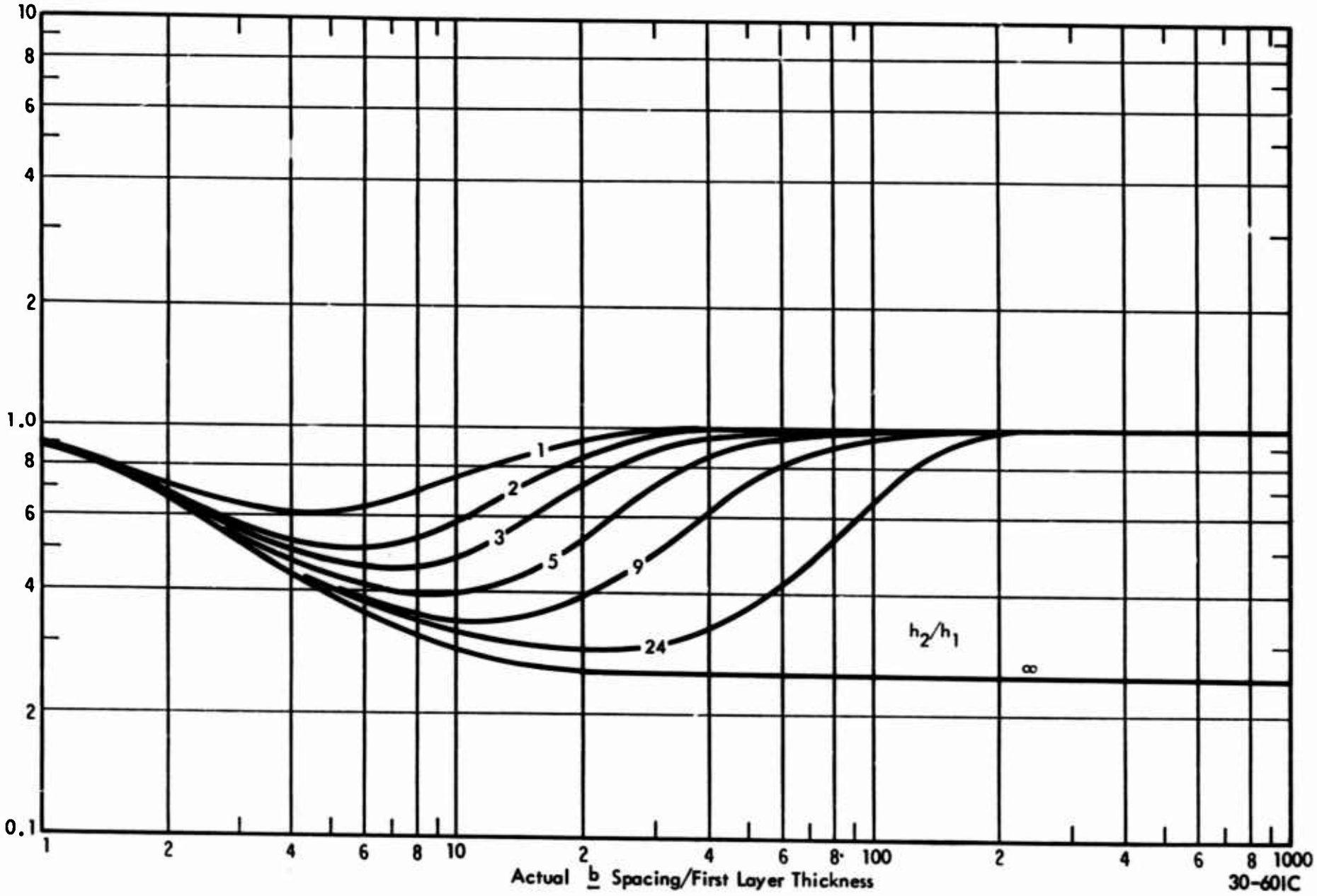

Figure A8 Broadside Array σ Sequence 1:1/4:1

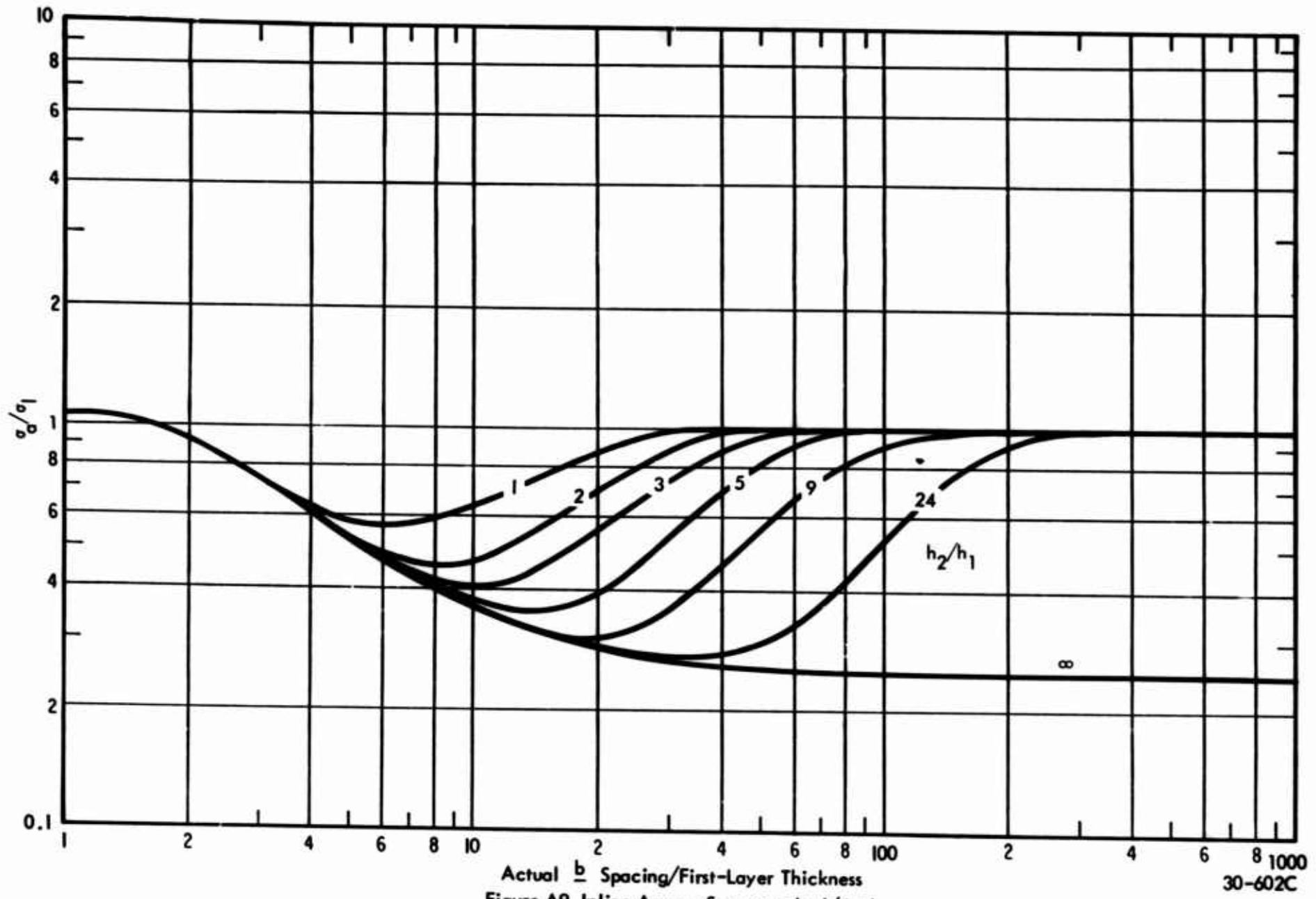

Figure A9 Inline Array σ Sequence 1 : 1/4 : 1

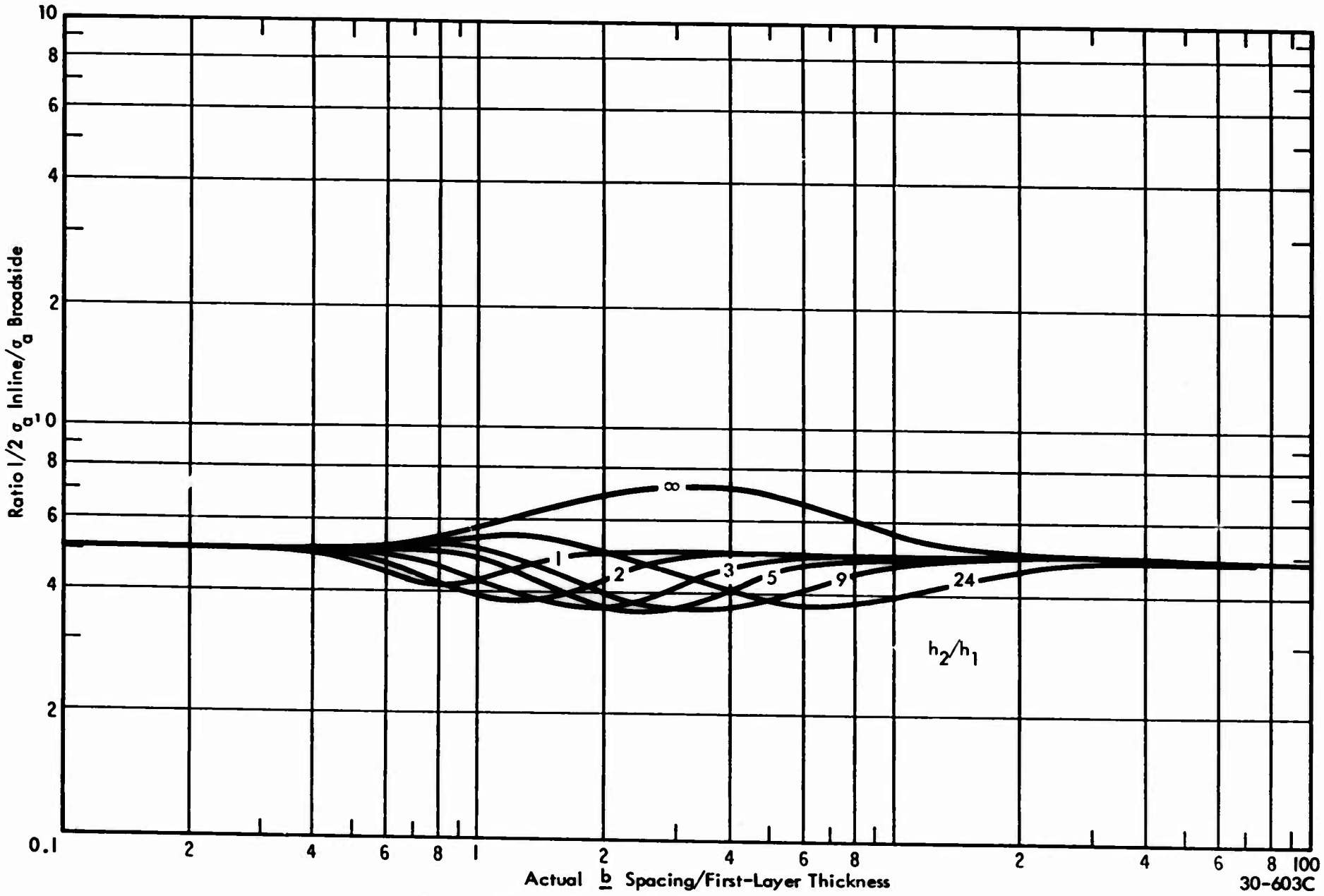

Figure A10 Ratio Curve 1/2 Inline: for σ Sequence 1:1/4:1

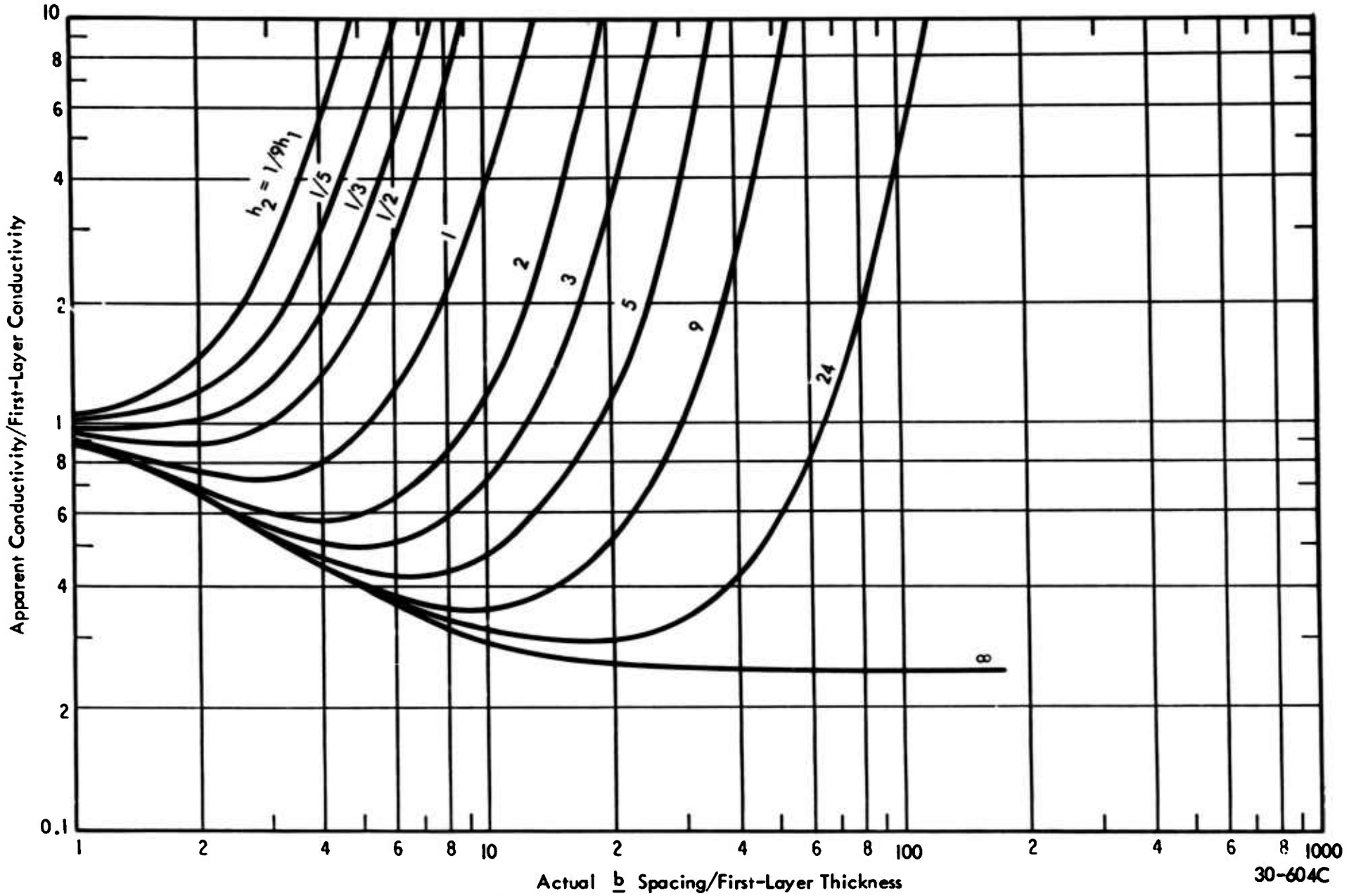

Figure All Broadside Array Sequence σ 1 : 1/4 : ∞

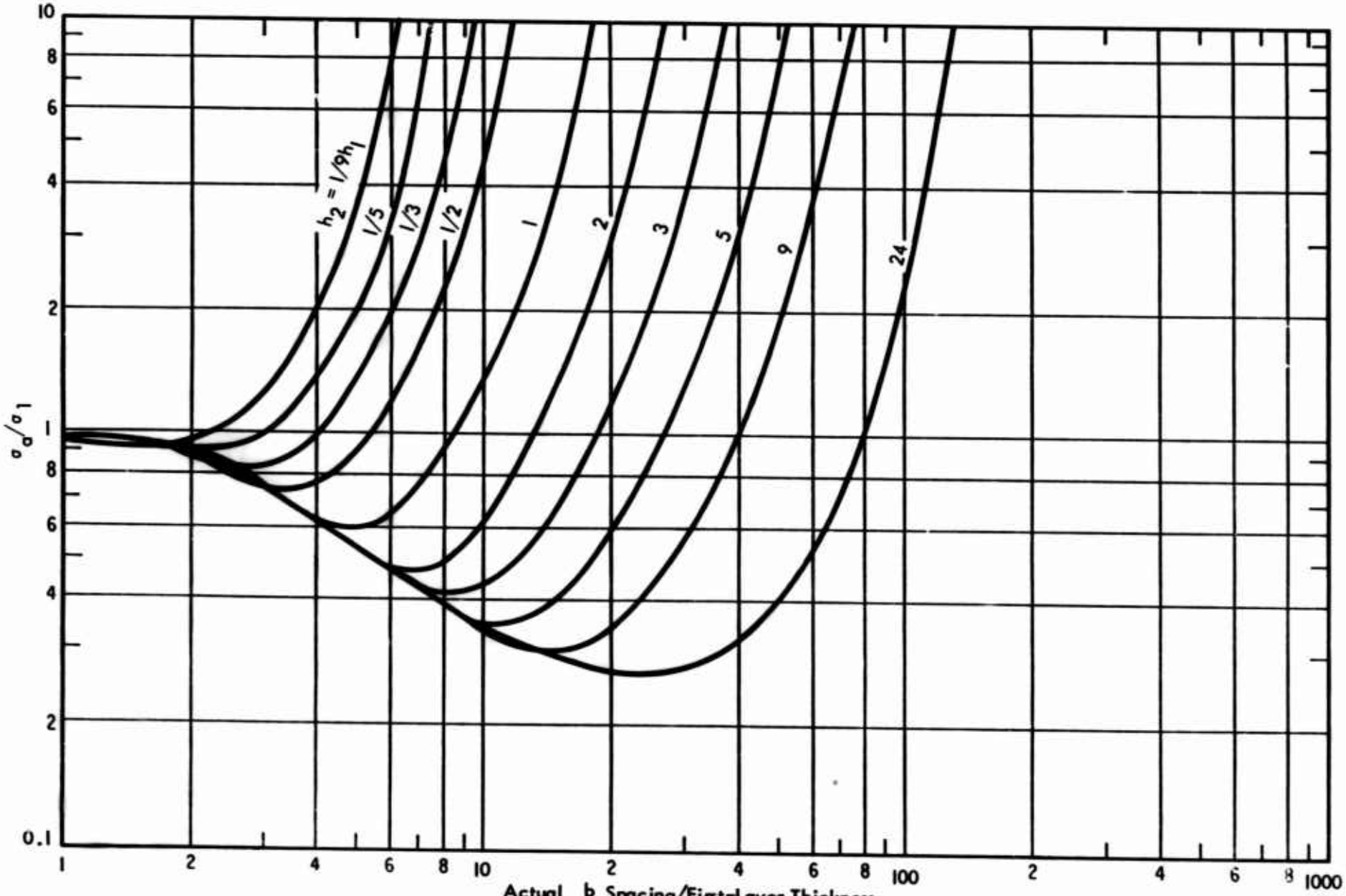

Figure A12 Inline Array Sequence of σ 1 : 1/4 : ∞

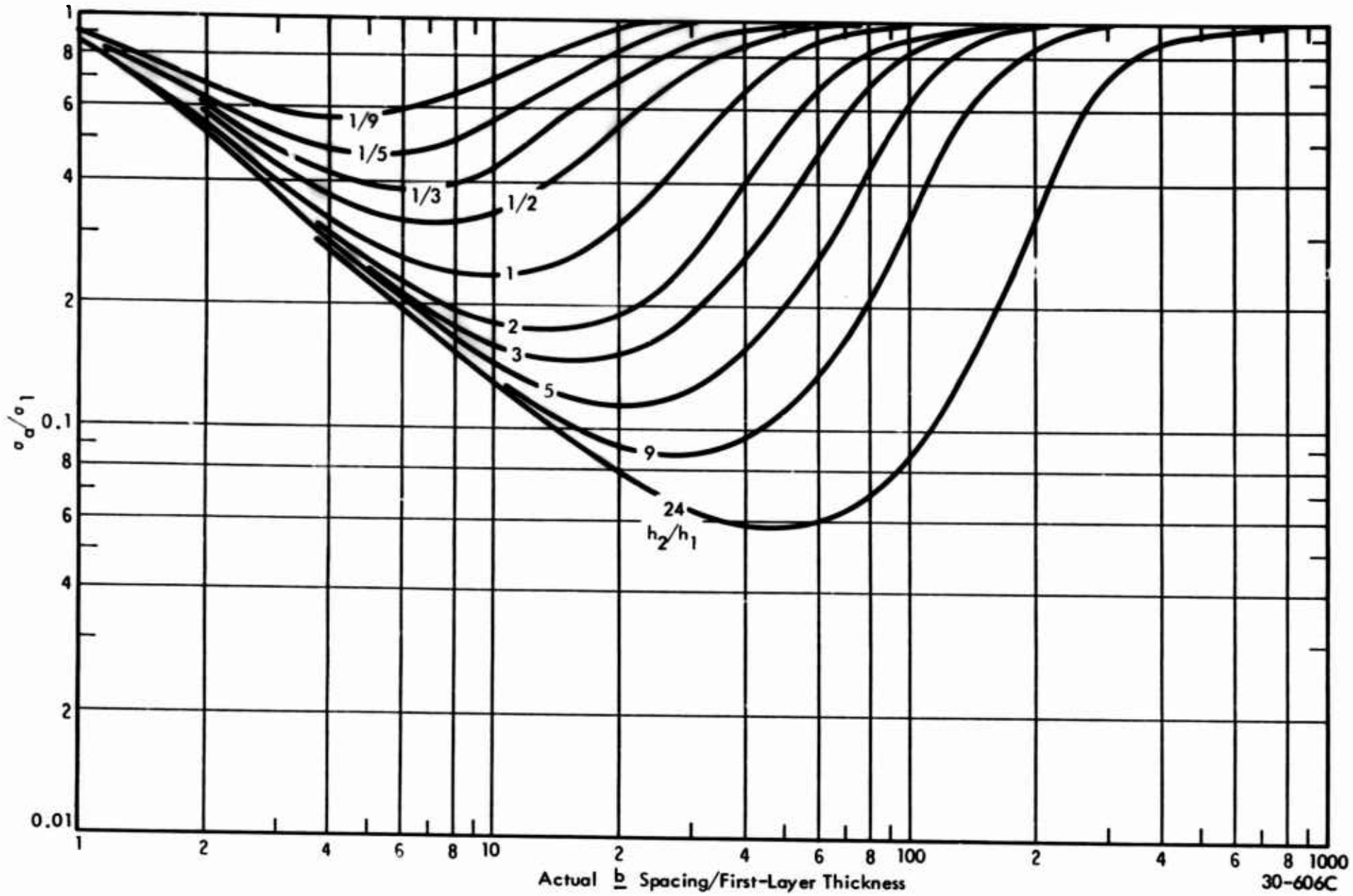

Figure A13 Broadside Array, σ Sequence 1:1/39:1

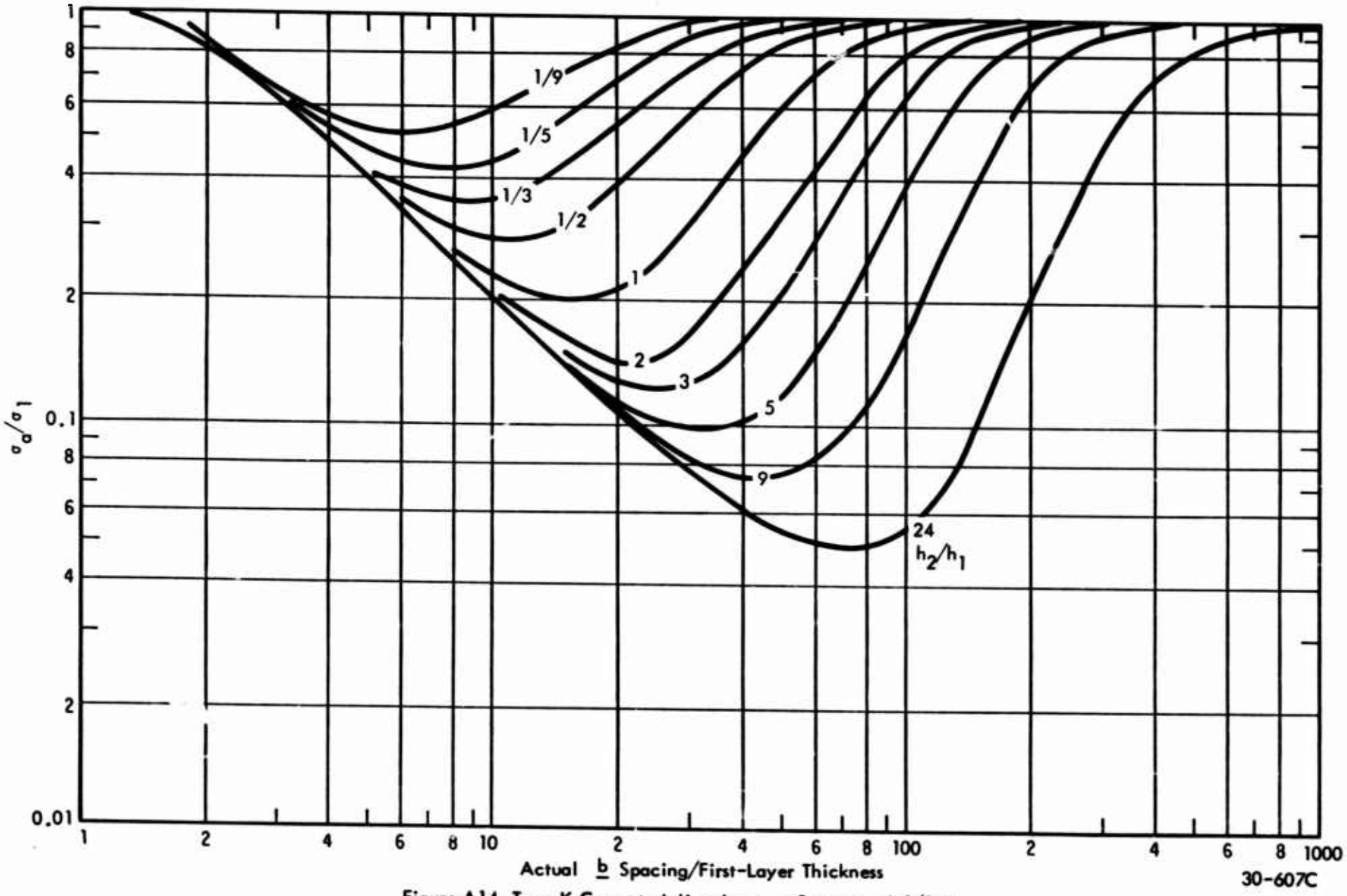

Figure A14 Type K Curve to Inline Array, σ Sequence 1:1/39:1

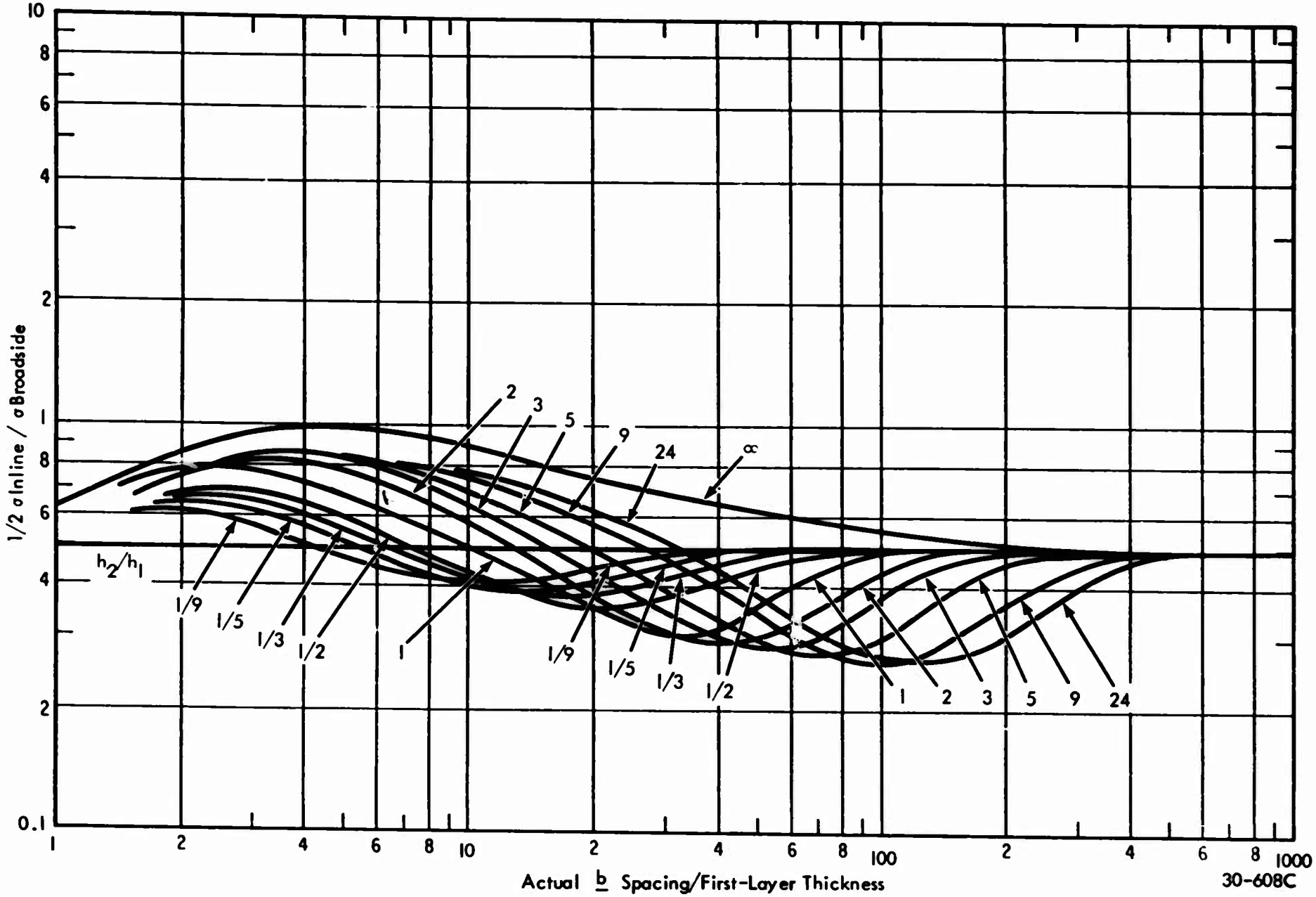

Figure A15 Ratio 1/2 Inline to Broadside for σ Sequence 1:1/39:1

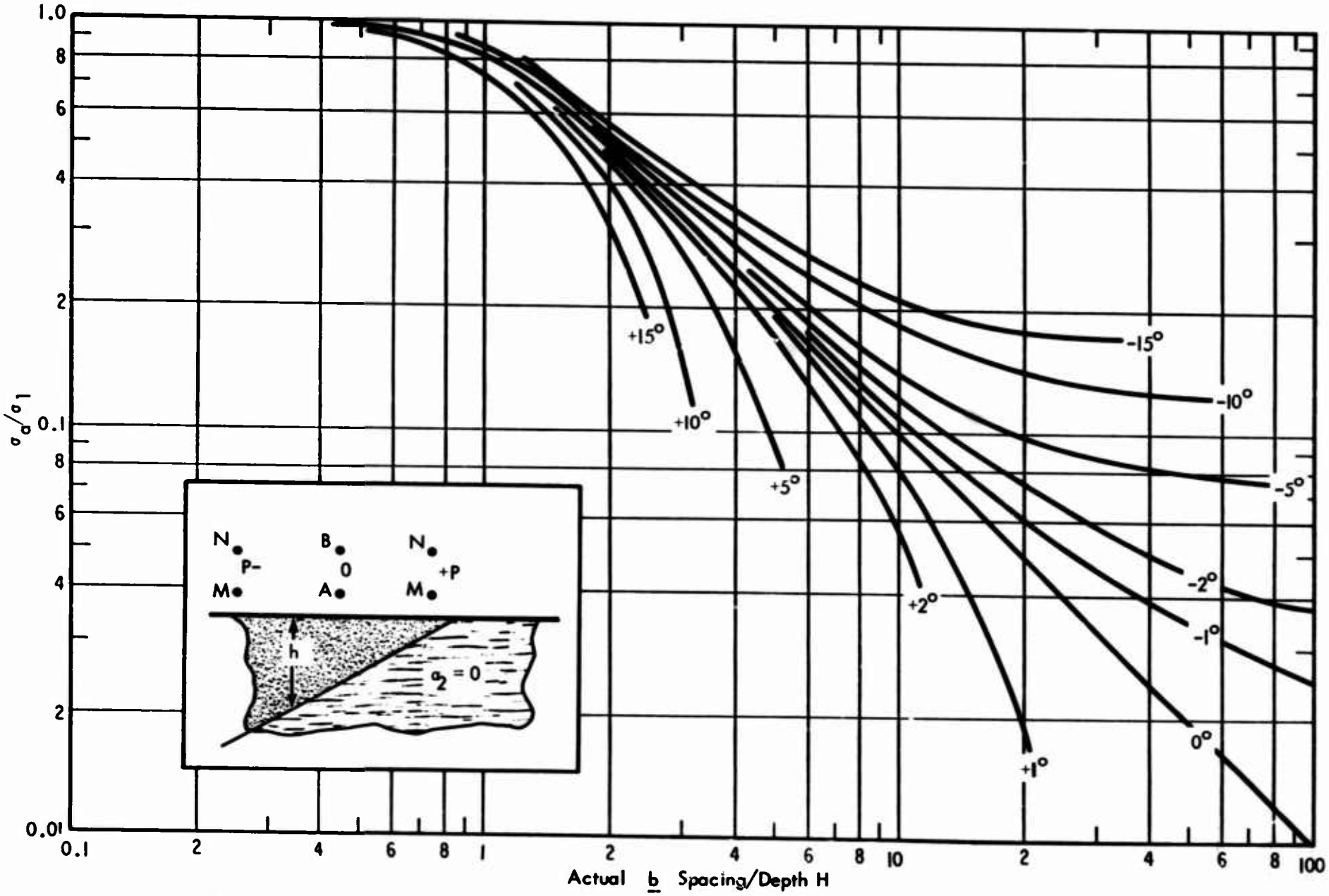

Figure A16 Broadside Dipping Insulator (Sign on Angle Refers to Direction of Expansion Relative to Dip)

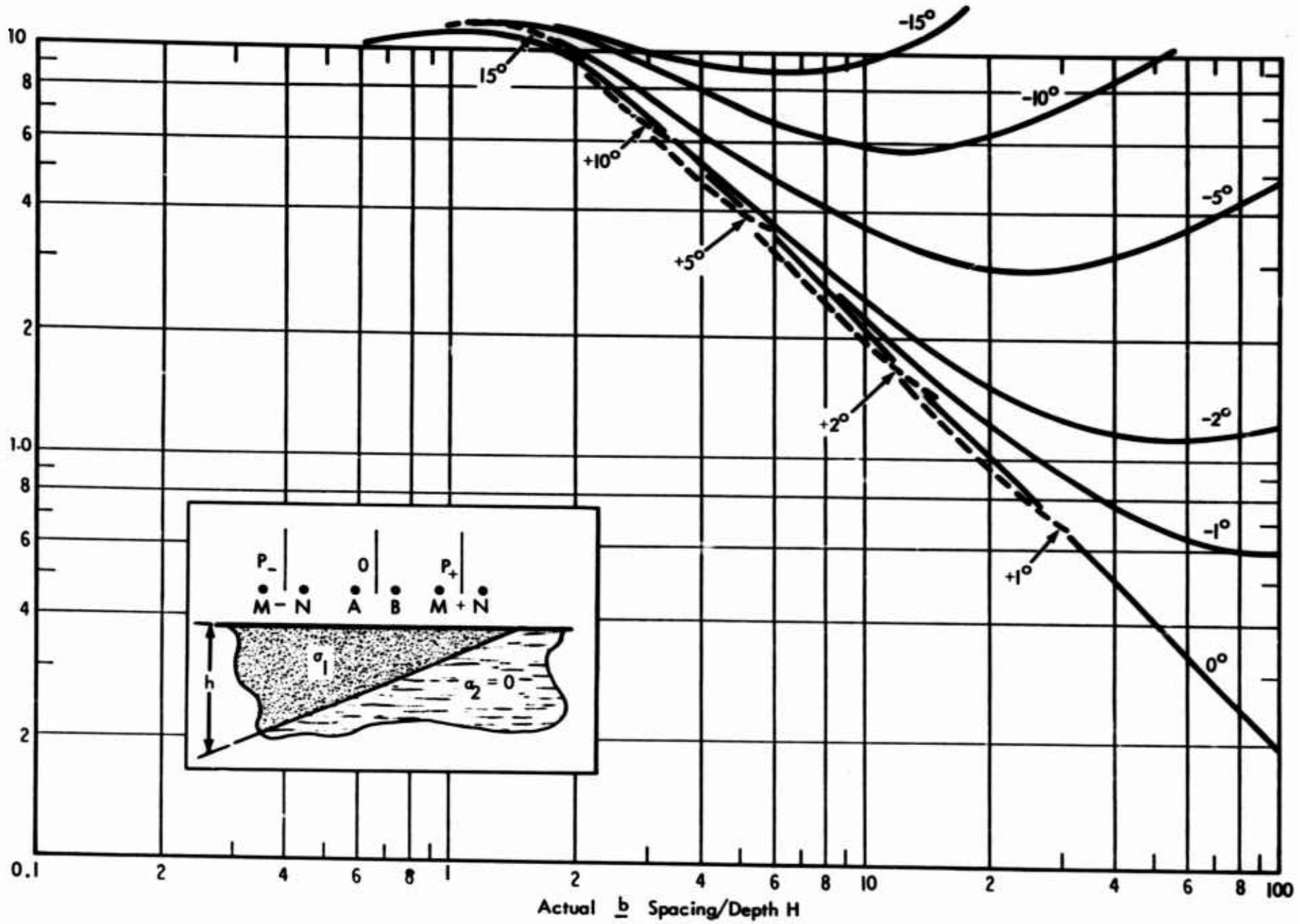

Figure A17 Inline (Polar) Dipping Insulator

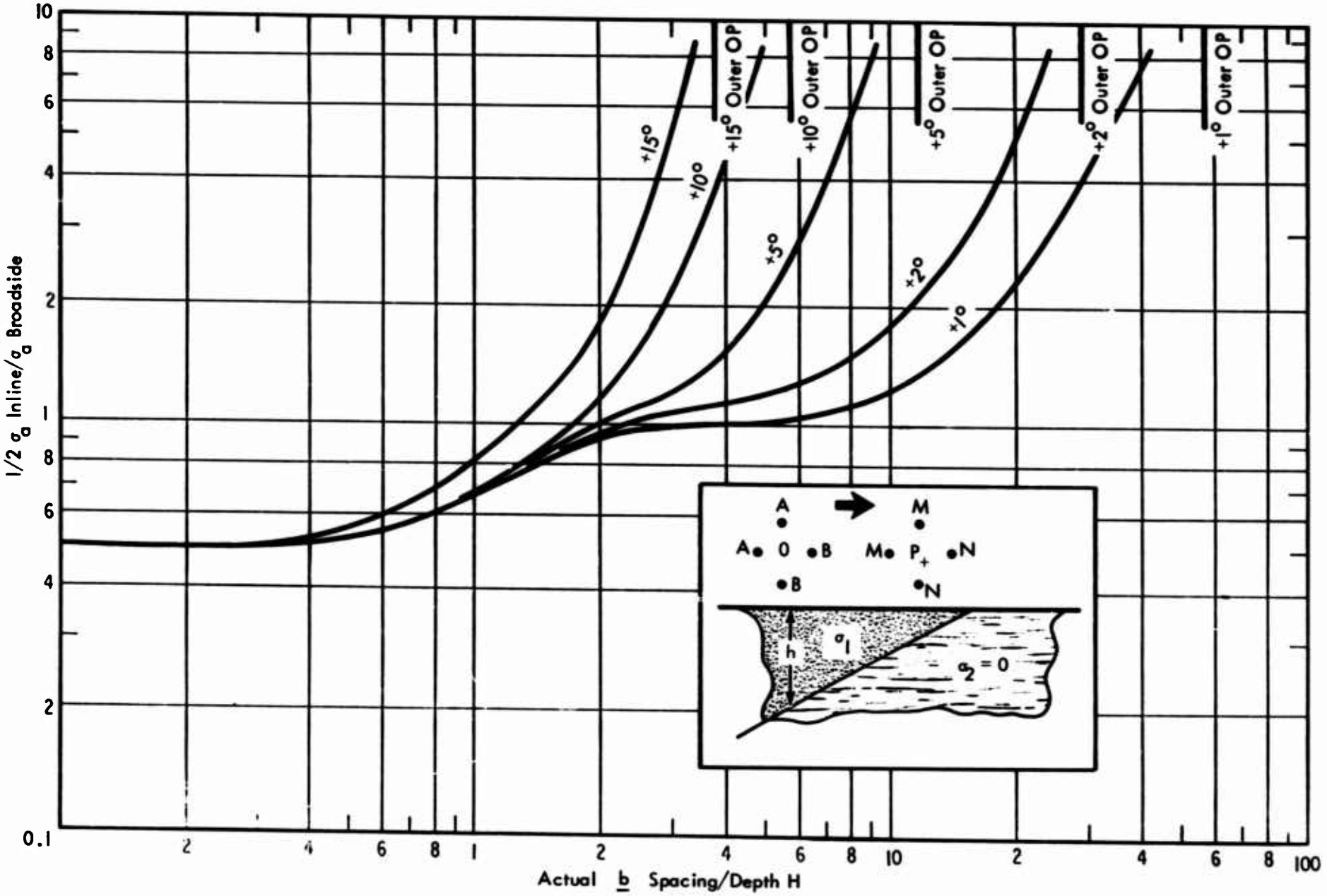

Figure A18 Ratio of 1/2 Inline to Broadside for Dipping Insulator (With Receiving Dipoles Moving Updip)

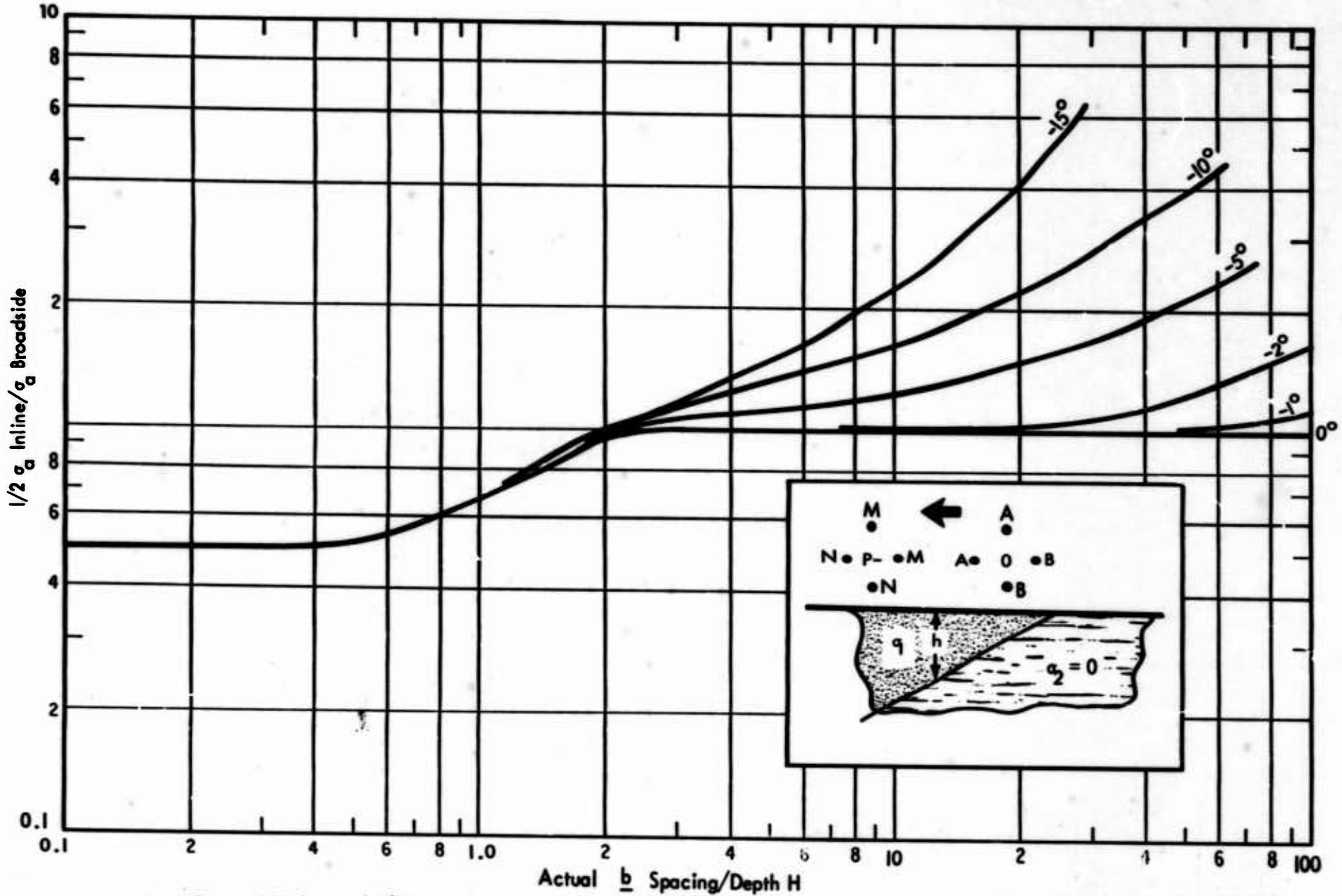

Figure A19 Ratio of 1/2 Inline to Broadside for Dipping Insulator (With Receiving Dipoles Moving Downdip)

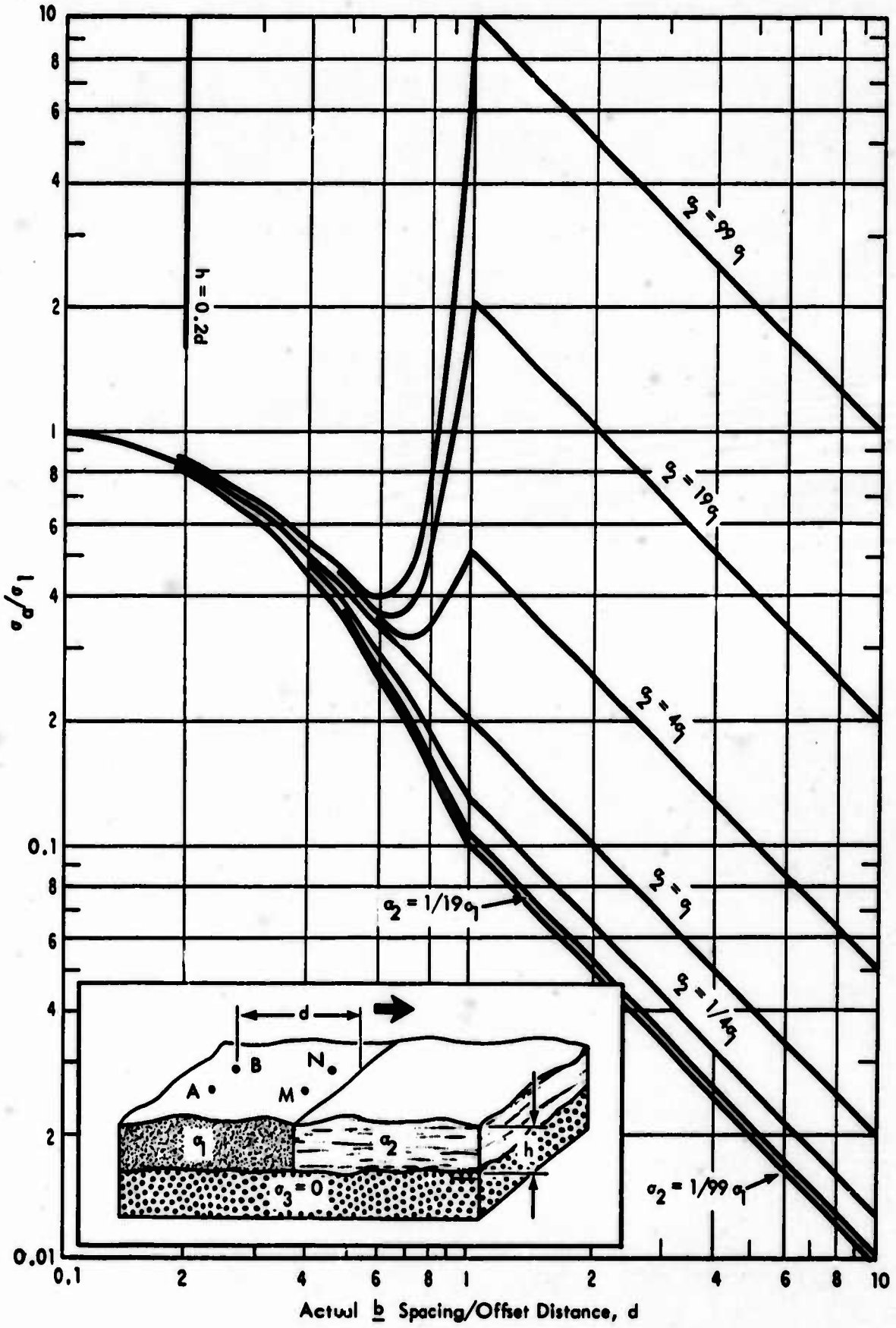

Figure A20 Lateral Change in Surface Conductivity, with the Receiving Dipole Crossing the Interface, for Broadside Array

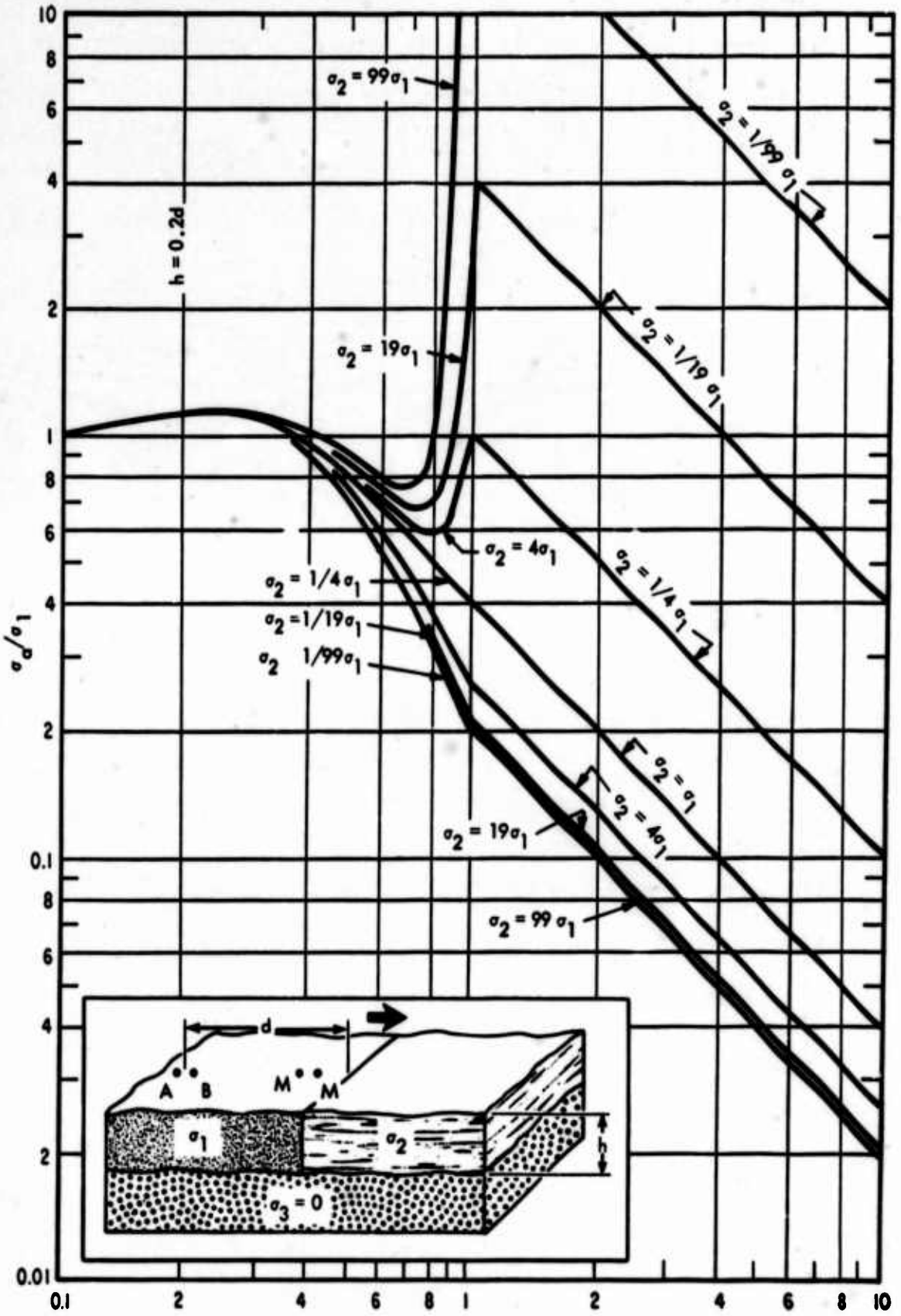

Figure A21 Lateral Change in Surface Conductivity, with the Receiving Dipole Crossing the Interface, for Inline Array

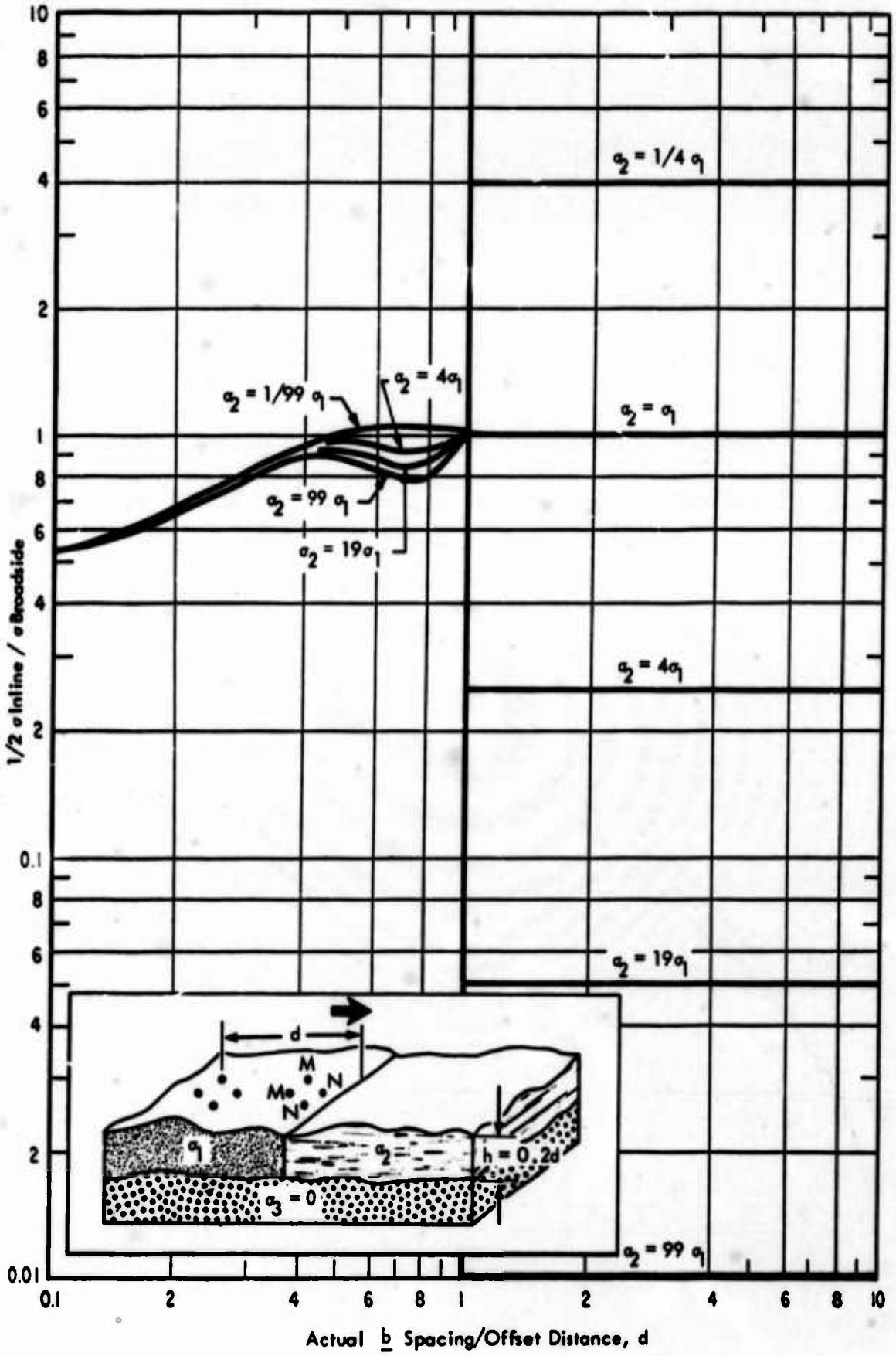

Figure A22 Lateral Change in Surface Conductivity with the Receiving Dipoles Crossing the Interface for Ratio of 1/2 Inline to Broadside

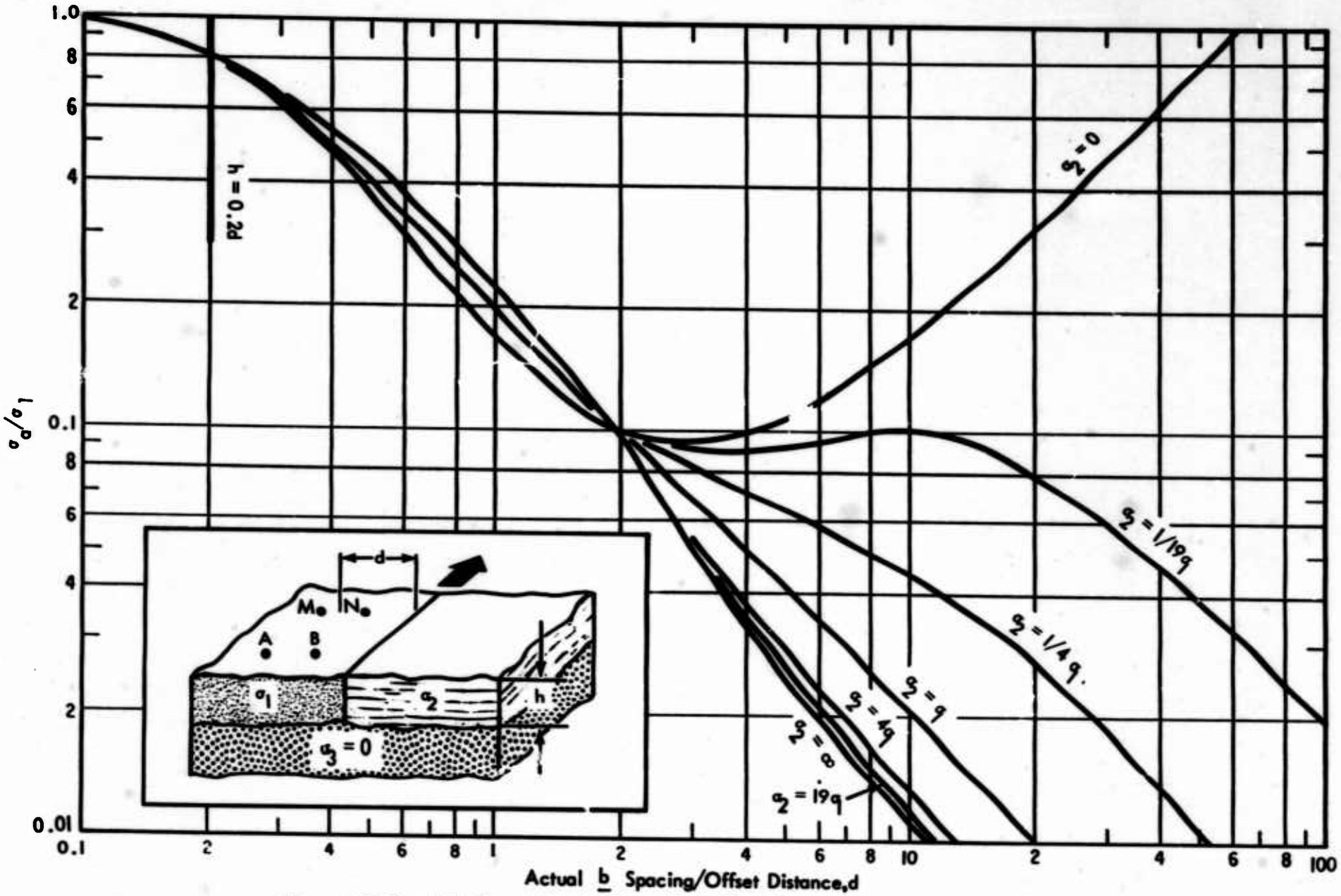

Figure A23 Broadside Array Lateral Change in Surface Conductivity Parallel to Expansion

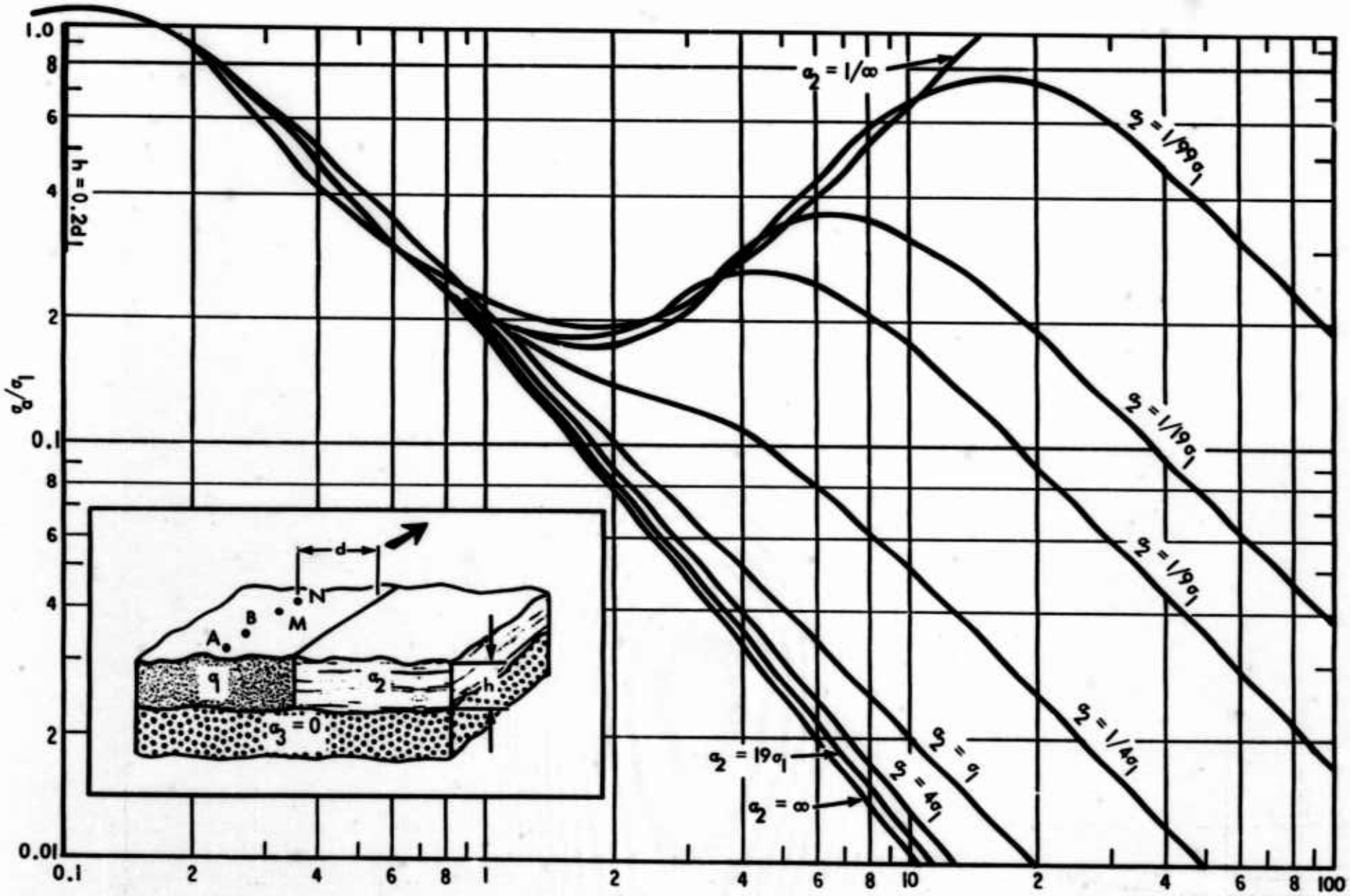

Figure A24 Inline, Expanded Parallel to Change in Surface Layer

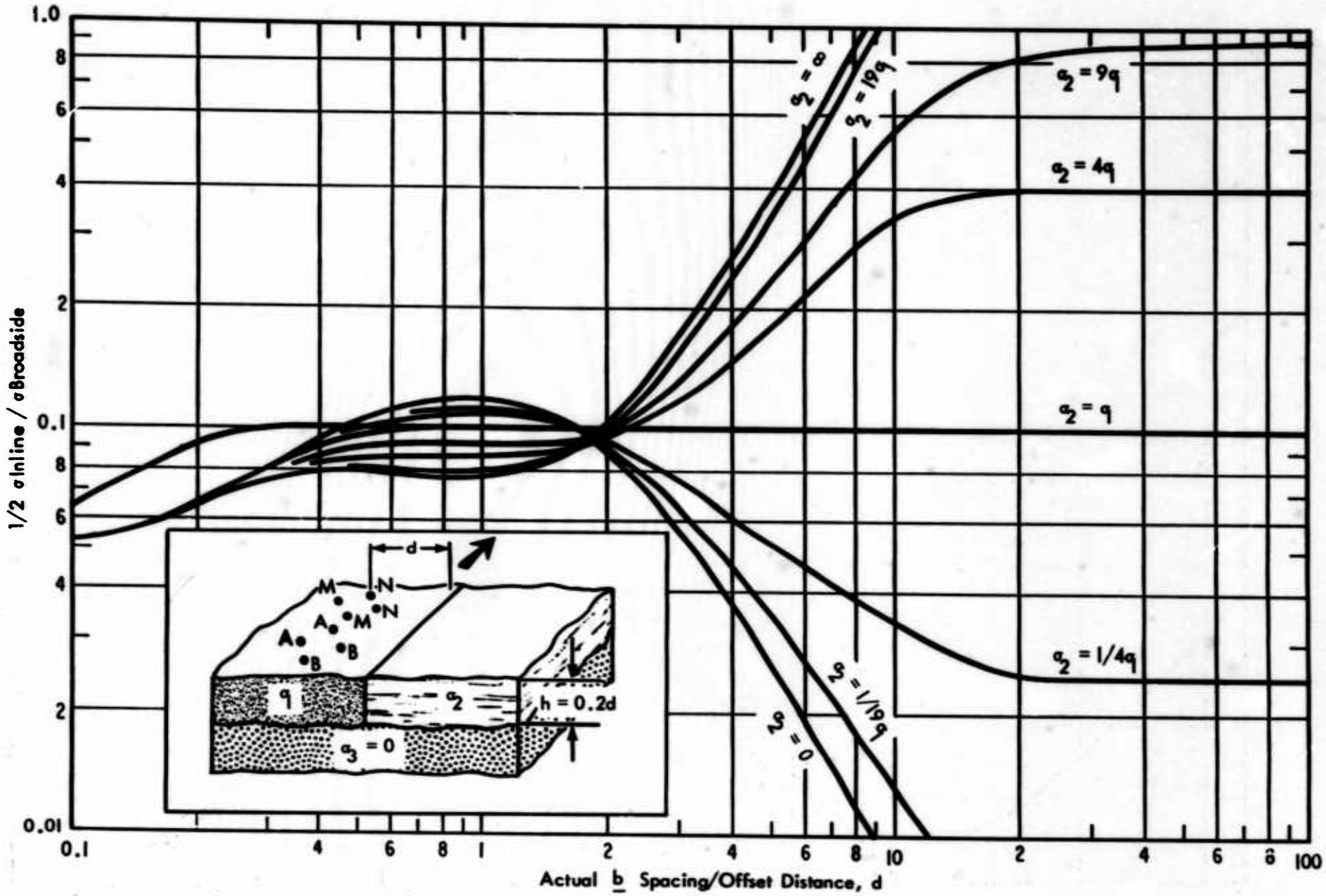

Figure A25 Ratio of 1/2 Inline to Broadside for Lateral Change in Surface Conductivity Parallel to Expansion

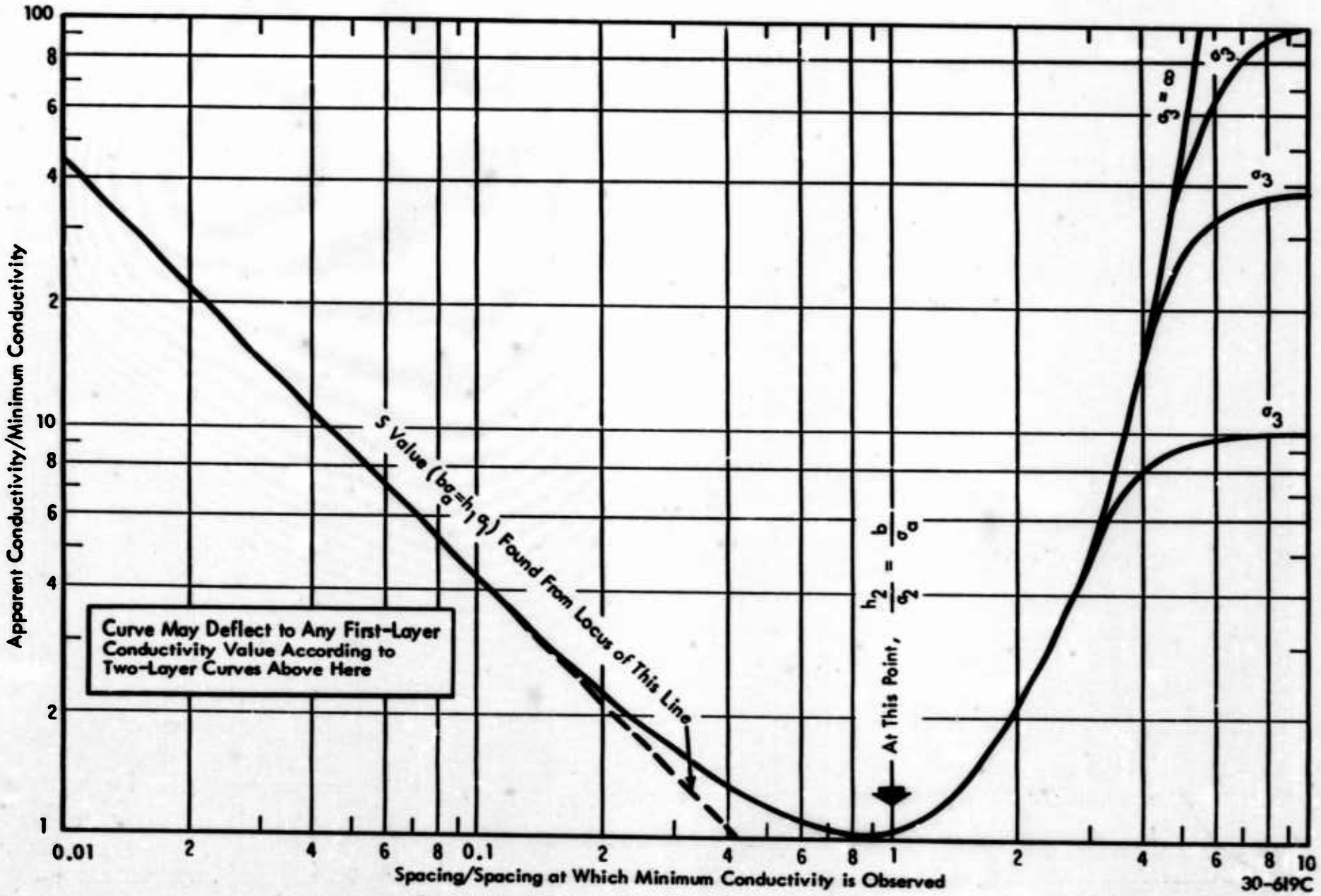

Figure A26 Broadside Array Three Layers σ_n = 1:0: ∞

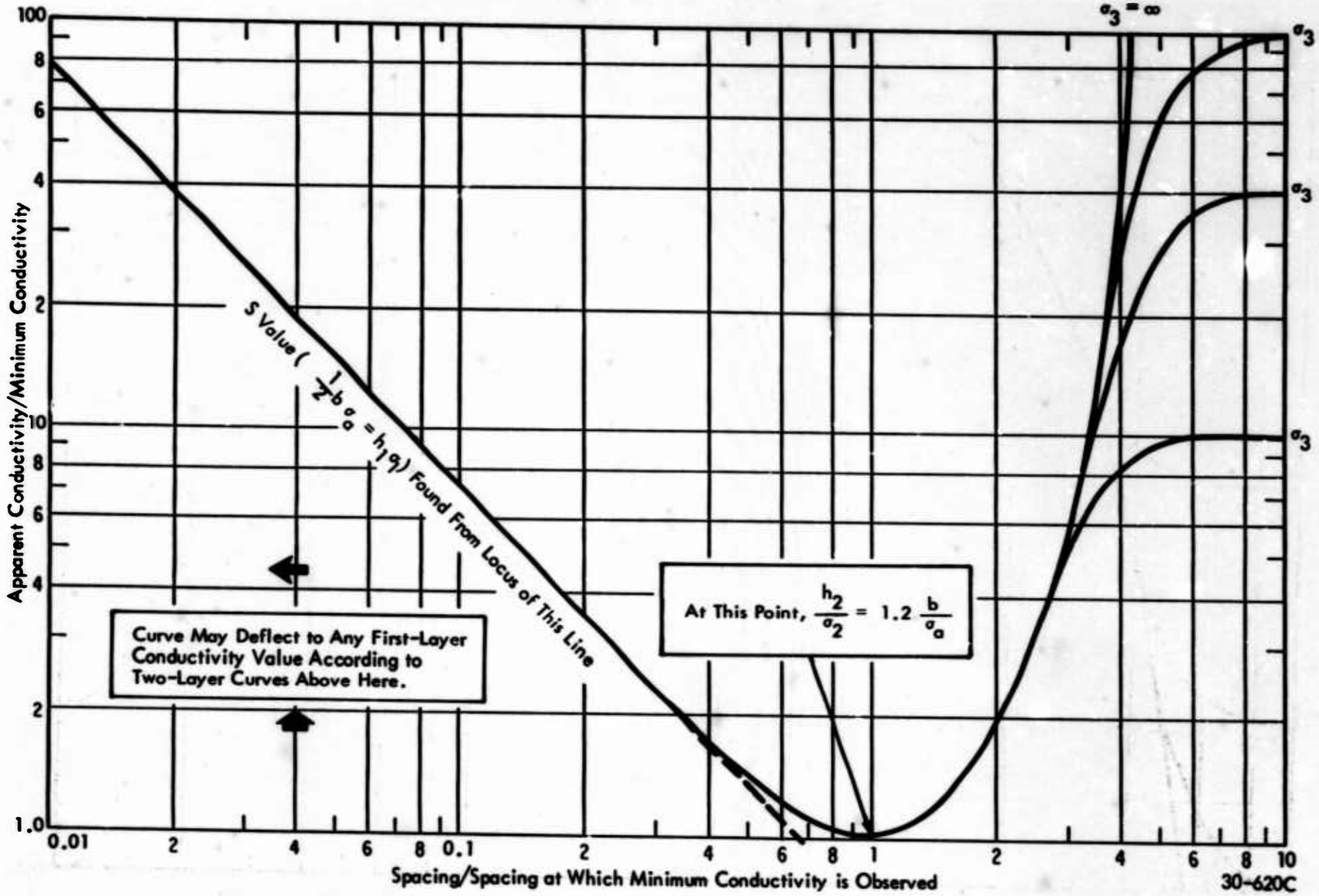

Figure A27 Inline Array Three Layers σ_n = 1:0:∞